Computers & Industrial Engineering 110 (2017) 462–483

Contents lists available at ScienceDirect

Computers & Industrial Engineering

journal homepage: www.elsevier.com/locate/caie

Sustainable network design for multi-purpose pellet processing depots under biomass supply uncertainty

Md Abdul Quddus [a], Niamat Ullah Ibne Hossain [a], Mohammad Marufuzzaman [a], Raed M. Jaradat [a,*], Mohammad S. Roni [b]

[a] Department of Industrial and Systems Engineering, Mississippi State University, PO Box 9542, MS 39762, United States
[b] Biofuel Computational Energy Analyst, Biofuels & Renewable Energy Technologies, Idaho National Laboratory, P.O. Box 1625, Idaho Falls, ID 83415, United States

ARTICLE INFO

Article history:
Received 13 November 2016
Received in revised form 21 April 2017
Accepted 3 June 2017
Available online 10 June 2017

Keywords:
Multi-purpose pellet processing depots
Densified biomass
Sample average approximation
Progressive hedging
Rolling horizon heuristic

ABSTRACT

This study develops a two-stage stochastic mixed-integer programming model to manage multi-purpose pellet processing depots under feedstock supply uncertainty. The proposed optimization model would help to minimize cost and mitigate emissions from the supply chain network. We consider three alternative Biomass Processing and Densification Depot (BPDD) technologies; namely, conventional pellet processing, high moisture pellet processing, and ammonia fiber expansion. These three technologies pre-process/pre-treat and densify different types of biomass into more highly densified intermediate products for different markets in order to improve movability and overall supply network performance in terms of costs and emissions. A hybrid decomposition algorithm was developed that combines Sample Average Approximation with an enhanced Progressive Hedging (PH) algorithm to solve this challenging $\mathcal{NP}$-hard problem. Some heuristics such as Rolling Horizon (RH) heuristic, variable fixing technique were later applied to further enhance the PH algorithm. Mississippi and Alabama were selected as a testing ground and ArcGIS was employed to visualize and validate the modeling results. The results of the analysis reveal promising insights that could lead to recommendations to help decision makers achieve a more cost-effective environmentally-friendly supply chain network.

1. Introduction

Bioenergy is considered to be a substitute source of energy that is necessary to help alleviate the reliance on petroleum energy. For decades, U.S. bioenergy production has depended heavily on conventional biomass supply systems. However, the current volatility in the crude oil market and the recent shutdown of some cellulosic bio-fuel plants necessitate the development of a more sustainable feedstock for future bio-economy growth. Feedstock can be defined as any renewable biological material including forest residue (wood), agricultural residue (corn-stover), and energy crops (switchgrass, miscanthus, sorghum). Feedstock developed for bioenergy could be made more sustainable if it had the flexibility to serve multiple markets in addition to bioenergy. Such markets could be bio-refineries, coal industries, pulp and paper industries, and animal feed markets (Bruglieri & Liberti, 2008; Vogel, Schmer, & Mitchell, 2010).

To develop a wide range of sustainable feedstocks, a biomass processing densification depot must be established in order to achieve a cost-effective outcome with the least risk. A Biomass Processing Densification Depot (BPDD) is a facility where biomass is densified into a stable feedstock to be supplied to larger facilities for energy production (Chai & Saffron, 2016; Parkhurst, Saffron, & Miller, 2016). BPDDs aggregate, store, moderately process and densify the biomass prior to delivering it to the bio-fuel markets. Although BPDD goals include such things as improving movability, derisking bio-refineries, increasing accessible resources, and enhancing quality control, the primary concerns of a BPDD system are to reduce material loss and to convert the low density biomass into a more stable, more densified product so that it can be transported over a much longer distance in a cost effective way (Eranki, Bals, & Dale, 2011; Rudolfsson, Stelte, & Lestander, 2015). Due to the diverse characteristics of biomass, various processes like grinding, densification, aggregating and mixing inside the depot produce a more uniform commodity that can be delivered to various markets in order to standardize the supply system. BPDD systems also increase the per acre utilization of biomass and enhance the usability of direct and indirect land use (Eranki et al., 2011). However,

* Corresponding author.
E-mail addresses: mq90@msstate.edu (M.A. Quddus), ni78@msstate.edu (N.U. Ibne Hossain), maruf@ise.msstate.edu (M. Mohammad), jaradat@ise.msstate.edu (R.M. Jaradat), mohammad.roni@inl.gov (M.S. Roni).

http://dx.doi.org/10.1016/j.cie.2017.06.001
0360-8352/

the seasonality and the yield variation of the biomass will directly impact the operation of a depot. For instance, the harvesting season for corn-stover starts in early September and ends in November, while woody biomass and miscanthus are available year round, except for three months in the winter. This seasonality not only impacts the operation of depot facilities for a given time period of the year but also affects the overall biomass supply chain activities. To address this challenge, supply chain managers need optimization models to decide where to locate depots and how to serve multiple markets (e.g., biorefinery, coal plants, pulp and paper industries, animal feed industries) under feedstock supply uncertainties. Three main alternative depots were identified to pre-process, treat, and densify different types of biomass into more highly densified intermediate products for different markets. The three main alternative depots are: conventional pelleting process, high moisture pelleting process, and ammonia fiber expansion.

Conventional Pelleting Process (CPP) and *High Moisture Pelleting Process* (HMPP) are conducted at standard depots whereas *Ammonia Fiber Expansion Process* (AFEX) is carried out at quality depot. A standard depot increases feedstock stability and storability and reduces material loss. In addition to the standard depot functions, a quality depot contains various processing steps such as chemical treatment, washing, hydrolysis, and leaching which help to reduce the pretreatment requirements at a client facility (Lamers et al., 2015). In a conventional pelleting process, pellets are reduced from their initial size to less than 50 mm rotary dried, and then sent for grinding to decrease particle size to less than 5 mm to meet particle size distribution requirements for pelleting (Lamers et al., 2015). Fig. 1 illustrates the steps involved in a conventional pelleting process (Lamers et al., 2015). CPP is selected to process forest residue that is transported to the depot in chip format (2–3 in.) for course size reduction through first stage grinding.

In a high moisture pelleting process (HMPP), high-moisture (30–35% MC) biomass is preheated and pelletized. In order to increase stability and reduce moisture content, final pellets are dried in a vertical grain dryer. These moderately dried pellets still contain high moisture content and require further drying so the moisture content falls below 9% to ensure safe storage and transportation. Fig. 2 illustrates the various unit operations associated with each step of HMPP (Lamers et al., 2015). An HMPP depot is suitable to handle the high moisture generated from herbaceous biomass (e.g., corn-stover, miscanthus) since it comes to the depot in a bale format.

The Ammonia Fiber Expansion (AFEX) process is fundamentally a dry to dry process since there is no watercourse produced during pretreatment (Teymouri, Laureano-Perez, Alizadeh, & Dale, 2005). AFEX ensures a higher conversion of different kinds of cellulosic biomass. Fig. 3 demonstrates the various unit operations associated with each step in a quality depot (Lamers et al., 2015). In the proposed model, the AFEX depot is selected to process corn-stover and miscanthus since AFEX pretreatment increases the glucan and xylan conversion making the biomass more attractive as a product for the animal feed market.

1.1. Related research

This section pursues two primary objectives. First, the current themes in the *biomass supply chain literature* are identified. The intent is to show some of the related methods used in biomass supply chain network and present the general thread running through these methods. Second, two main gaps are addressed in the literature. The focus is to address these two gaps by developing a two-stage stochastic mixed-integer linear programming (MILP) model

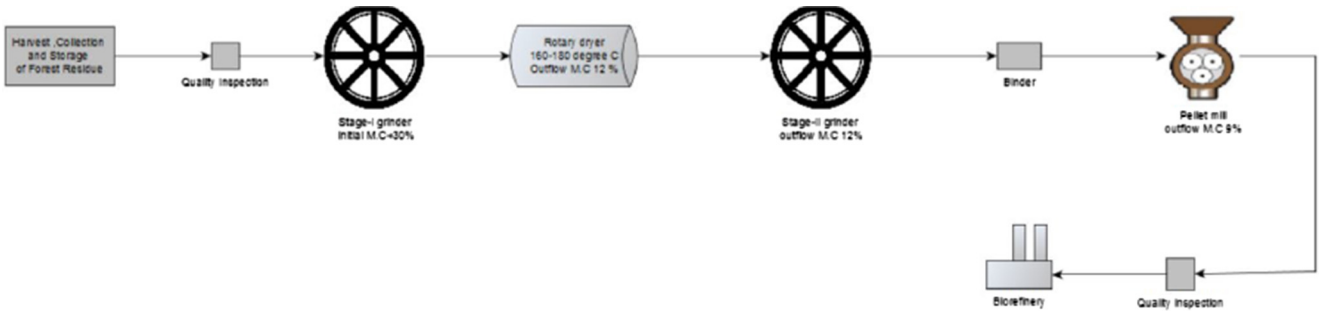

Fig. 1. Conventional Pelleting Process (CPP) flow diagram.

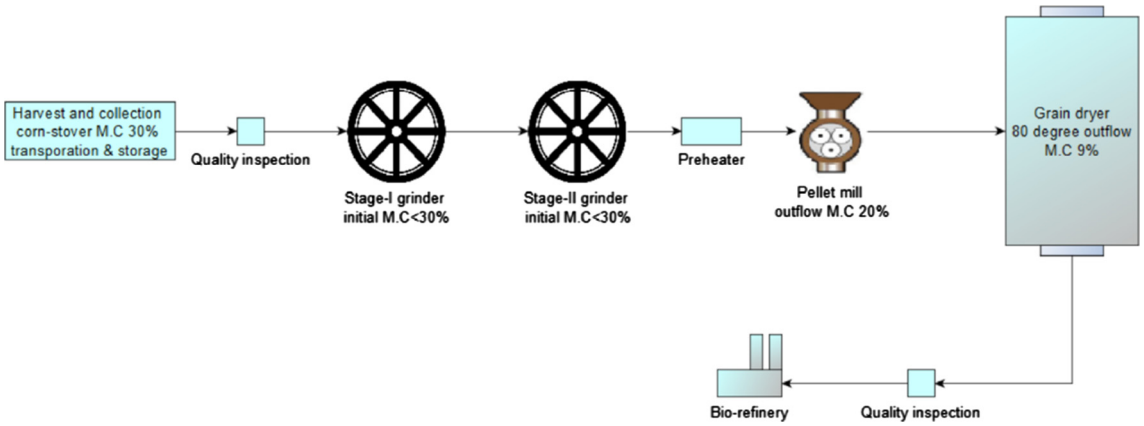

Fig. 2. High Moisture Pelleting Process (HMPP) flow diagram.

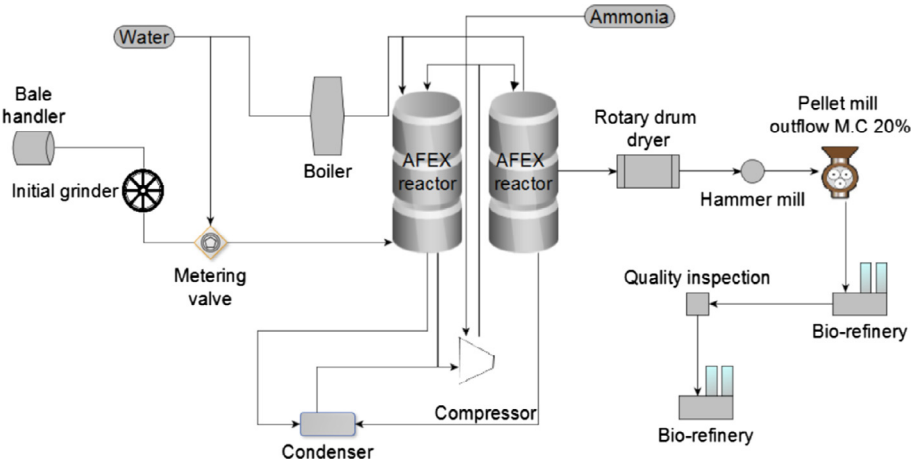

Fig. 3. Ammonia Fiber Expansion (AFEX) process flow diagram.

to design and manage a sustainable *multi-purpose pellet processing depots* under feedstock seasonality fluctuations and uncertainty.

1.1.1. Current themes in the literature

The purpose of this subsection is to provide a synthesis of the main contribution and themes of the current research in the literature as well as the current limitations and gaps.

The proper design of the biomass supply chain network is one of the most significant and challenging phases of bio-fuel production (Kim, Realff, Lee, Whittaker, & Furtner, 2011). In recent years, research pertaining to supply chain optimization networks for biomass and bio-fuel systems has flourished. Various models and solutions have been developed and analyzed to determine the optimal locations of supply sites, depots, and bio-fuel markets. While some studies were conducted to integrate strategic and tactical level supply chain network decisions (e.g., An, Wilhelm, & Searcy, 2011; Huang, Chen, & Fan, 2010), others used deterministic settings and focused on plant location and transportation issues (e.g., Eksioglu, Acharya, Leightley, & Arora, 2009; Roni, Eksioglu, Searcy, & Jha, 2014; Memisoglu et al., in press; Xie & Ouyang, 2013).

The previous studies were extended to develop more capable optimization models that could handle complexity and uncertainties exhibited in bio-fuel supply chain networks (e.g., Awudu & Zhang, 2013; Gebreslassie, Yao, & You, 2012; Kim, Realff, & Lee, 2011; Marufuzzaman, Eksioglu, & Huang, 2014). Although stochastic models provide reliable solutions, they are less represented in the literature due to the need of additional computational burden and difficulties in developing solution algorithms. A brief overview of studies dedicated to uncertainty and sustainability in a biofuel supply chain network can be found in a recent study by Awudu and Zhang (2012). Many researchers labelled *facility reliability* and *network sustainability* as main concerns in bio-fuel supply chain networks and highlighted the impact of network sustainability and facility reliability on bio-fuel supply chain networks (e.g., Li, Peng, Bai, & Ouyang, 2015; Marufuzzaman, Li, Yu, & Zhou, 2016; Poudel, Marufuzzaman, & Bian, 2016b).

The literature pertaining to general network designing problem that adopts a two-stage stochastic programming approach is ample. For instance, Atamturk and Zhang (2007) and Barbarosoglu and Arda (2004) developed a two-stage stochastic programming model that considers multi-commodities and vulnerability of commodity sources under demand uncertainty. Kara and Onut (2010) developed a two-stage stochastic programming model that examines the reconstruction of a reversed supply chain network design for a real-world paper recycling company. In the same vein, Simic (2016) developed an interval-parameter two-stage stochastic full-infinite programming approach for the management of the allocation of end-of-life vehicles by capturing uncertainties in crisp intervals and probability distributions. Interested readers can review a number of recently solved network designing problems that adopted two-stage stochastic programming approach, including Qi and Sen (2017), Poudel, Marufuzzaman, and Bian (2016a), Marufuzzaman et al. (2014), Zhang, Johnson, and Wang (2016), and others. Besides these modeling techniques, a number of decomposition algorithms are proposed to solve these two-stage stochastic programming models, such as L-shaped method (Rajgopal, Wang, Schaefer, & Prokopyev, 2011), progressive hedging (PH) algorithm (Huang, Fan, & Chen, 2014), sample average approximation (Santoso, Ahmed, Goetschalckx, & Shapiro, 2005), an integration of the above techniques (Schutz, Tomasgard, & Ahmed, 2009), and many others.

Another theme found in the literature focuses on developing methods and techniques to minimize feedstock uncertainties and biomass processing depot costs (e.g., Dutta et al., 2011; Hess, Wright, Kenney, & Searcy, 2009). Lamers et al. (2015) conducted a comparison of depot costs and advantages across bio-refinery supply chains by applying techno-economic analysis of decentralized biomass processing depots. Similarly, Bals and Dale (2012) established a flexible techno-economic model of local biomass processing depots (LBPD) that could assess profitability in multiple scenarios of biomass processing with different technologies. Eranki et al. (2011) in another study, explored the concepts of regional biomass processing depots, their features, benefits and potential challenges. Argo et al. (2013) indicated that supply sites, depots and bio-fuel markets can be constructed in different sites including lower yield areas. With another study, Carolan, Joshi, and Dale (2007) conducted a technical and financial feasibility analysis of distributed bioprocessing using regional biomass preprocessing depots to minimize the transportation, transaction and storage cost of feedstock. Along the same line, Eranki and Dale (2011) extended the previous study by performing a comparative life cycle assessment (LCA) of distributed and centralized biomass processing systems. Another study by Ng and Maravelias (2015) proposed a mixed-integer non-linear programming model to solve the capacity and inventory planning problem of biofuels supply chain including depots. The authors further developed in Ng and Maravelias (2017) a mixed-integer linear programming (MILP) model for biomass selection and allocation, technology assortment, and capacity planning at regional depots. An optimization model considering RBPDs that explicitly integrates resiliency in the objective function for maximizing profit is developed by

Maheshwari, Singla, and Shastri (2017). Based on some heuristics rules, Li, Li, Varbanov, and Liu (2017) exploited the applications of the distance potential (sum of the distance from the source to demand point or sum of the distance from the depot to demand point) to the design of regional biomass supply chains and solving vehicle routing problem. Stemming from a review of the literature, Table 1 provides a synthesis of the current themes in the biomass supply chain literature. These general themes serve as a baseline in developing the proposed model.

1.1.2. Current gaps in the literature

After surveying the literature two significant gaps are identified and need to be addressed to improve and foster the body of knowledge in biomass supply chain network. These gaps are:

- No optimization framework is proposed in the literature to design a *multipurpose pellet processing depot-based* biomass supply chain network considering the complex interactions that exist between consumer markets (e.g., coal plants, bio-refineries) and depots.
- Lack of research studied the impact of feedstock seasonality and uncertainty on bio-fuel markets and biomass consumer markets (e.g., coal plants) with different locations and configuration of depots.

In summary, this study proposes a two-stage stochastic mixed-integer linear programming (MILP) model to design and manage a sustainable multi-purpose pellet processing depots under feedstock seasonality and uncertainty. The design of the proposed stochastic model should be robust to include bio-refineries and other related markets such as pulp and paper industries, animal feed industries, and coal plants. We seek to identify the complex interactions that exist between the sustainable multi-purpose pellet processing depots with different biomass consumer markets by developing a real world case scenario. Further, experiments such as impact of biomass supply variations and stochasticity, emission policies and quotas are made to understand the impact of these key parameters on a multi-purpose depot based biomass supply chain network. All the experimental results are visualized and validated by developing a real-world case study using data from the states of Mississippi and Alabama.

We realized that solving this proposed depot-based biomass supply chain network model is challenging due to the presence of NP-hardness facility location problem structure. Therefore, we propose a hybrid decomposition algorithm that combines Sample Average Approximation with an enhance Progressive Hedging (PH) algorithm to solve this challenging problem. The PH algorithm is enhanced through the application of rolling horizon and variable fixing techniques. Computational experiments reveal that the proposed decomposition algorithm is capable of solving realistic size problem instances with high quality in a reasonable amount of time. The insights gained from the computational experiments can lead to recommendations to help decision makers achieve a more sustainable, economic, and environmentally-friendly feedstock supply chain network.

This paper is organized as follows: Section 2 presents the two-stage stochastic programming model formulation; Section 3 outlines the developed hybrid solution approach to solve the proposed optimization model, and Section 4 describes the results deduced from a series of performed computational experiments. The paper concludes with future research and implications.

Table 1
Current themes of the bio-fuel supply network literature.

Authors	General themes
An et al. (2011) and Huang et al. (2010)	Development of models that integrate strategic as well as tactical level decisions pertaining to biomass supply chain network
Eksioglu et al. (2009), Xie and Ouyang (2013), Roni et al. (2014), and Memisoglu et al. (in press)	Development of deterministic models to handle supply chain drivers (facility and transportation decisions)
Kim et al. (2011), Gebreslassie et al. (2012), Awudu and Zhang (2013), and Marufuzzaman et al. (2014)	Development of stochastic biofuel supply chain models to understand network complexities and uncertainties
Li et al. (2015), Marufuzzaman et al. (2016), and Poudel et al. (2016b)	Emphasis on the need to study facility reliability and network sustainability in bio-fuel supply chain
Atamturk and Zhang (2007), Barbarosoglu and Arda (2004), Kara and Onut (2010), and Simic (2016)	Development of two-stage stochastic models to study general characteristics of supply chain network (i.e., commodities and management of bio fuel supply network)
Hess et al. (2009), Dutta et al. (2011), Eranki et al. (2011), and Eranki and Dale (2011)	Development of economic models to minimize depot costs, feedstock uncertainties to improve bio-fuel life cycle cost
Lamers et al. (2015), Bals and Dale (2012), and Carolan et al. (2007)	Implementation of technologies into the bio-fuel supply chain network
Ng and Maravelias (2015, 2017)	Development of non-linear models to handle capacity and inventory planning decisions in biofuel supply chain network

2. Problem description and model formulation

The main objective of this paper is to build a two-stage stochastic programming model to aid the design and management of sustainable pellet processing depots so that they can meet multiple market demands while taking into account the stochastic nature of the feedstock supply. The problem consists of selecting a set of depots among candidate locations and determining the routes of feedstock flow from various supply sites to different market locations. The mathematical model can minimize total system costs and reduce carbon emissions. In the two-stage stochastic programming model formulation, the first-stage, which should occur prior to the realization of any random events, is to decide from among the possible candidates the one with the most promising location and capacity to open *Biomass Processing and Densification Depots* (BPDDs). After the first-stage decisions are made, the random events are realized and the second-stage decisions such as the cost of procuring, storing, and transporting biomass from feedstock supply sites to markets are taken. The object of the model is to minimize the first-stage and expected second-stage costs across all possible feedstock supply scenarios for the biomass supply chain network. Fig. 4 illustrates the structure of a simplified BPDDs supply chain network consisting of three supplier sites, three depots, and four markets. The mathematical model is described below.

Let $\mathbb{G}(\mathscr{N},\mathscr{A})$, denotes a logistics network where $\mathscr{N}$ is the set of nodes and $\mathscr{A}$ is the set of arcs. Set $\mathscr{N}$ consists of the set of harvesting sites $\mathscr{I}$, the set of candidate depots $\mathscr{J}$, and the set of markets $\mathscr{K}$, i.e., $\mathscr{N}=\mathscr{I}\cup\mathscr{J}\cup\mathscr{K}$. In order to distinguish between different feedstock harvesting sites, set $\mathscr{I}$ further partitioned into three different subsets: $\mathscr{I}_w$ represents the set of nodes supplying forest residues; $\mathscr{I}_c$ represents the set of nodes supplying corn-stover; $\mathscr{I}_m$ represents the set of nodes supplying miscanthus and $\mathscr{I}=\mathscr{I}_w\cup\mathscr{I}_c\cup\mathscr{I}_m$. Similarly, set $\mathscr{A}$ can be partitioned into two disjoint subsets i.e., $\mathscr{A}=\mathscr{A}_1\cup\mathscr{A}_2$ where $\mathscr{A}_1$ represents the set of arcs connecting harvesting sites $\mathscr{I}$ with depots $\mathscr{J}$ and $\mathscr{A}_2$ represents

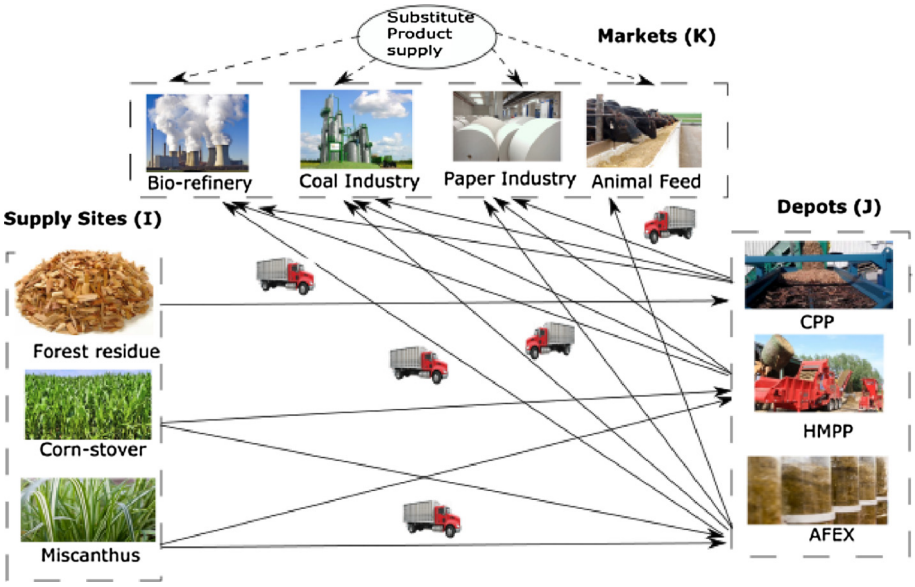

Fig. 4. Network representation of a feedstock supply chain.

the set of arcs connecting depots $\mathscr{J}$ with markets $\mathscr{K}$. Locating a depot of capacity $l \in \mathscr{L}$ of type $m \in \mathscr{M}$ at each location $j \in \mathscr{J}$ costs a fixed set-up cost ψ_{lmj} and generates a production of capacity c^{cap}_{lmj} and holding capacity h^{cap}_{lmj}. Transportation distances along arcs $(i,j) \in \mathscr{A}$ are relatively short; therefore, trucks are preferred to ship biomass along these arcs and its unit transportation costs are denoted by c_{bijt} and c_{jkt}. Let $\mathscr{B}$ represent the set of different feedstock types (e.g., forest residues, corn-stover, and miscanthus) and $\mathscr{T}$, the set of time periods. Finally, Ω denotes the sample space of the random event where $\omega \in \Omega$ defines a particular realization.

Let s^{ω}_{bit} denote the amount of biomass of type $b \in \mathscr{B}$ available in harvesting site $i \in \mathscr{I}$ at time $t \in \mathscr{T}$ under scenario $\omega \in \Omega$ and d_{kt} as the demand in each market $k \in \mathscr{K}$ which is required to be met at time period $t \in \mathscr{T}$. The proposed model assumes that the unmet demand for feedstock at each market location $k \in \mathscr{K}$ can be satisfied with a substitute product by paying a penalty cost of π_{kt}. The penalty cost implies that if the cost of delivering feedstock through the internal supply chain exceeds this threshold cost, then the demand for feedstock will be satisfied through the substitute product. We now make the following assumptions to simplify our modeling approach:

Assumption 1. The physical structure of a supply chain consists of feedstock harvesting, collection and storage by the individual farmer, individual farmer or farmers co-op societies, transporting the raw materials to the depot, and depot conversion of the low density biomass into more stable densified products (increase bulk density) and delivering it to different markets.

Assumption 2. We hypothesize that CPP will process forest residue that will be transported to the depot in chip format (2–3 in.) for coarse size reduction. Processed forest residue from CPP depot can be supplied to all markets but animal feed markets.

Assumption 3. We have considered that an HMPP depot is suitable to handle the high moisture generated from herbaceous biomass (e.g., corn-stover, miscanthus) since it comes to the depot in a bale format. Processed corn-stover and miscanthus from HMPP depots serves all markets except animal feed.

Assumption 4. In the proposed model, the AFEX depot can also process corn-stover and miscanthus since AFEX pretreatment increases the glucan and xylan conversion making the biomass more beneficial as a commercial product to supply for all types of markets.

Assumption 5. Transportation distances along arcs are relatively short; therefore, trucks are preferred to ship biomass along these arcs.

Assumption 6. The proposed model assumes that the unmet demand for feedstock at each market location can be satisfied with a substitute product by paying a penalty cost. The penalty cost implies that if the cost of delivering feedstock through the internal supply chain exceeds this threshold cost, then the demand for feedstock will be satisfied through the substitute product.

Assumption 7. If there is an overflow in biomass supply (i.e., high realization) and the depot owners do not need to purchase them all, it is assumed that the unsold biomass will be considered as "lost" sale from the farmers' side.

Following these notations, we summarize the sets and input parameters for the two-stage stochastic programming formulation:

Sets:

- $\mathscr{I}_w$: set of suppliers for forest residues
- $\mathscr{I}_c$: set of suppliers for corn-stover
- $\mathscr{I}_m$: set of suppliers for miscanthus
- $\mathscr{I}$: set of all feedstock supply sites, i.e., $\mathscr{I} = \mathscr{I}_w \bigcup \mathscr{I}_c \bigcup \mathscr{I}_m$
- $\mathscr{B}$: set of feedstock types (b_1 for forest residues, b_2 for corn-stovers, b_3 for miscanthus, i.e., $\mathscr{B} = \{b_1, b_2, b_3\}$)
- $\mathscr{J}_w$: set of CPP depots
- $\mathscr{J}_c$: set of HMPP depots
- $\mathscr{J}_m$: set of AFEX depots
- $\mathscr{J}$: set of all depots, i.e., $\mathscr{J} = \mathscr{J}_w \bigcup \mathscr{J}_c \bigcup \mathscr{J}_m$
- $\mathscr{M}$: set of depot types (M_1 for CPP which process only forest residues, M_2 for HMPP which process corn-stover and miscanthus, M_3 for AFEX which also process corn-stovers and miscanthus, i.e., $\mathscr{M} = \{M_1, M_2, M_3\}$)

- $\mathscr{K}_b$: set of markets for bio-refinery
- $\mathscr{K}_c$: set of markets for coal industries
- $\mathscr{K}_p$: set of markets for pulp and paper industries
- $\mathscr{K}_a$: set of markets for animal feed industries
- $\mathscr{K}$: set of all market, i.e., $\mathscr{K} = \mathscr{K}_b \bigcup \mathscr{K}_c \bigcup \mathscr{K}_p \bigcup \mathscr{K}_a$
- $\mathscr{T}$: set of time periods
- $\mathscr{L}$: set of capacities
- Ω: set of scenarios

Parameters:

- ψ_{ljm}: fixed cost of opening a depot of type $m \in \mathscr{M}$ with capacity $l \in \mathscr{L}$ at location $j \in \mathscr{J}$
- c_{bijt}: unit cost of transporting feedstock of type $b \in \mathscr{B}$ along arc $(i,j) \in \mathscr{A}_1$ at time period $t \in \mathscr{T}$
- c_{jkt}: unit cost of transporting densified biomass along arc $(j,k) \in \mathscr{A}_2$ at time period $t \in \mathscr{T}$
- s^{ω}_{bit}: amount of feedstock of type $b \in \mathscr{B}$ available at site $i \in \mathscr{I}$ in time period $t \in \mathscr{T}$ under scenario $\omega \in \Omega$
- d_{kt}: feedstock demand in market $k \in \mathscr{K}$ at time period $t \in \mathscr{T}$
- c^{s}_{lmj}: feedstock storage/handling capacity of size $l \in \mathscr{L}$ for depot type $m \in \mathscr{M}$ in location $j \in \mathscr{J}$
- c^{p}_{lmj}: densified feedstock production capacity of size $l \in \mathscr{L}$ for depot type $m \in \mathscr{M}$ in location $j \in \mathscr{J}$
- h^{cap}_{lmj}: feedstock holding capacity of size $l \in \mathscr{L}$ for depot type $m \in \mathscr{M}$ at location $j \in \mathscr{J}$
- σ_{bit}: unit procurement cost for feedstock of type $b \in \mathscr{B}$ in location $i \in \mathscr{I}$ at time period $t \in \mathscr{T}$
- h_{jt}: unit depot holding cost in depot $j \in \mathscr{J}$ at time period $t \in \mathscr{T}$
- p_{jt}: unit densified feedstock production cost for depot type $m \in \mathscr{M}$ located at $j \in \mathscr{J}$ in time period $t \in \mathscr{T}$
- γ: average expected cost of carbon credits ($/ton)
- e^{1}_{bijt}: emission due to per unit feedstock of type $b \in \mathscr{B}$ transporting from supply site $i \in \mathscr{I}$ to depot $j \in \mathscr{J}$ in time period $t \in \mathscr{T}$
- e^{2}_{bjt}: emission due to per unit of densified feedstock of type $b \in \mathscr{B}$stored in location $j \in \mathscr{J}$ at time period $t \in \mathscr{T}$
- e^{3}_{jkt}: emission due to per unit feedstock transporting from depot in location $j \in \mathscr{J}$ to market $k \in \mathscr{K}$ at time period $t \in \mathscr{T}$
- ϕ_b: conversion rate from feedstock (tons/tons) to densified feedstock of type $b \in \mathscr{B}$
- α_b: deterioration rate of feedstock of type $b \in \mathscr{B}$
- $\overline{CO_{2t}}$: maximum amount of carbon dioxide (CO_2) (in tons) that are permitted to emit in time period $t \in \mathscr{T}$ (allocated by the government)
- π_{kt}: unit penalty cost of not satisfying market demand at location $k \in \mathscr{K}$ in time period $t \in \mathscr{T}$
- ρ_{ω}: probability of scenario $\omega \in \Omega$

Decision variables:

- Y_{lmj}: 1 if a depot type $m \in \mathscr{M}$ of capacity $l \in \mathscr{L}$ is opened in location $j \in \mathscr{J}$; 0 otherwise
- H^{ω}_{bjt}: amount of feedstock of type $b \in \mathscr{B}$ stored in location $j \in \mathscr{J}$ at time period $t \in \mathscr{T}$ under scenario $\omega \in \Omega$
- X^{ω}_{bijt}: amount of feedstock of type $b \in \mathscr{B}$ transported from supply site $i \in \mathscr{I}$ to depot $j \in \mathscr{J}$ at time period $t \in \mathscr{T}$ under scenario $\omega \in \Omega$
- X^{ω}_{jkt}: amount of densified biomass transported from location $j \in \mathscr{J}$ to market $k \in \mathscr{K}$ at time period $t \in \mathscr{T}$ under scenario $\omega \in \Omega$
- W^{ω}_{bjt}: amount of feedstock of type $b \in \mathscr{B}$ processed in location $j \in \mathscr{J}$ at time period $t \in \mathscr{T}$ under scenario $\omega \in \Omega$
- CO^{ω}_{2t}: amount of carbon dioxide (CO_2) that is currently emitted (in tons) at time period $t \in \mathscr{T}$ under scenario $\omega \in \Omega$
- U^{ω}_{kt}: amount of biomass shortage in market $k \in \mathscr{K}$ at time period $t \in \mathscr{T}$ under scenario $\omega \in \Omega$

We now introduce the following first and second-stage decision variables for the proposed two-stage stochastic programming model formulation. The first stage decision variables $\mathbf{Y} := \{Y_{lmj}\}_{l\in\mathscr{L},m\in\mathscr{M},j\in\mathscr{J}}$ determine the size, type, and location to open a depot, i.e.,

$$Y_{lmj} = \begin{cases} 1 & \text{if a depot of size } l \text{ of type } m \text{ is used at location } j \\ 0 & \text{otherwise;} \end{cases}$$

The second-stage decision variables $\mathbf{X} := \{X^{\omega}_{bmnt}\}_{b\in\mathscr{B},(m,n)\in\mathscr{A},t\in\mathscr{T},\omega\in\Omega}$ denote the flow of feedstock of type $b \in \mathscr{B}$ along each link $(m,n) \in \mathscr{A}$ of the network at time period $t \in \mathscr{T}$ under scenario $\omega \in \Omega$; $\mathbf{H} := \{H^{\omega}_{bjt}\}_{b\in\mathscr{B},j\in\mathscr{J},t\in\mathscr{T},\omega\in\Omega}$ decide the amount of feedstock stored in depot $j \in \mathscr{J}$ at time period $t \in \mathscr{T}$ under scenario $\omega \in \Omega$; $\mathbf{W} := \{W^{\omega}_{bjt}\}_{b\in\mathscr{B},j\in\mathscr{J},t\in\mathscr{T},\omega\in\Omega}$ decide the amount of feedstock of type $b \in \mathscr{B}$ processed at depot $j \in \mathscr{J}$ in time period $t \in \mathscr{T}$ under scenario $\omega \in \Omega$, and finally $\mathbf{U} := \{U^{\omega}_{kt}\}_{k\in\mathscr{K},t\in\mathscr{T},\omega\in\Omega}$ decide the amount of feedstock shortage at market location $k \in \mathscr{K}$ in time period $t \in \mathscr{T}$ under scenario $\omega \in \Omega$. With this, we are now ready to formulate the following two-stage stochastic mixed-integer linear programming model referred to as **[DP]**:

$$[\mathbf{DP}] \underset{\mathbf{Y,X,H,W,U}}{Minimize} \sum_{l\in\mathscr{L}}\sum_{m\in\mathscr{M}}\sum_{j\in\mathscr{J}} \psi_{lmj} Y_{lmj} + \sum_{t\in\mathscr{T}}\sum_{\omega\in\Omega} \rho_{\omega} \left(\sum_{b\in\mathscr{B}}\sum_{i\in\mathscr{I}}\sum_{j\in\mathscr{J}} (c_{bijt} + \sigma_{bit}) X^{\omega}_{bijt} + \sum_{j\in\mathscr{J}}\sum_{k\in\mathscr{K}} (c_{jkt} + p_{jt}) X^{\omega}_{jkt} + \sum_{b\in\mathscr{B}}\sum_{j\in\mathscr{J}} h_{jt} H^{\omega}_{bjt} + \sum_{k\in\mathscr{K}} \pi_{kt} U^{\omega}_{kt} \right) \quad (1)$$

Subject to

$$\sum_{j\in\mathscr{J}} X^{\omega}_{bijt} \leqslant s^{\omega}_{bit} \quad \forall b \in \mathscr{B},\ i \in \mathscr{I},\ t \in \mathscr{T},\ \omega \in \Omega \quad (2)$$

$$\sum_{i\in\mathscr{I}} X^{\omega}_{bijt} + (1-\alpha_b) H^{\omega}_{bjt-1} = H^{\omega}_{bjt} + W^{\omega}_{bjt} \quad \forall b \in \mathscr{B},\ j \in \mathscr{J},\ t \in \mathscr{T},\ \omega \in \Omega \quad (3)$$

$$\sum_{b\in\mathscr{B}} H^{\omega}_{bjt} \leqslant \sum_{l\in\mathscr{L}} h^{cap}_{lmj} Y_{lmj} \quad \forall m \in \mathscr{M},\ j \in \mathscr{J},\ t \in \mathscr{T},\ \omega \in \Omega \quad (4)$$

$$\sum_{k\in\mathscr{K}} X^{\omega}_{jkt} \leqslant \sum_{b\in\mathscr{B}} \phi_b W^{\omega}_{bjt} \quad \forall j \in \mathscr{J},\ t \in \mathscr{T},\ \omega \in \Omega \quad (5)$$

$$\sum_{b\in\mathscr{B}} W^{\omega}_{bjt} \leqslant \sum_{l\in\mathscr{L}} c^{s}_{lmj} Y_{lmj} \quad \forall m \in \mathscr{M},\ j \in \mathscr{J},\ t \in \mathscr{T},\ \omega \in \Omega \quad (6)$$

$$\sum_{k\in\mathscr{K}} X^{\omega}_{jkt} \leqslant \sum_{l\in\mathscr{L}} c^{p}_{lmj} Y_{lmj} \quad \forall m \in \mathscr{M},\ j \in \mathscr{J},\ t \in \mathscr{T},\ \omega \in \Omega \quad (7)$$

$$\sum_{j\in\mathscr{J}} X^{\omega}_{jkt} + U^{\omega}_{kt} = d_{kt} \quad \forall k \in \mathscr{K},\ t \in \mathscr{T},\ \omega \in \Omega \quad (8)$$

$$\sum_{l\in\mathscr{L}}\sum_{m\in\mathscr{M}} Y_{lmj} \leqslant 1 \quad \forall j \in \mathscr{J} \quad (9)$$

$$Y_{lmj} \in \{0,1\} \quad \forall l \in \mathscr{L},\ m \in \mathscr{M},\ j \in \mathscr{J} \quad (10)$$

$$X^{\omega}_{bijt},\ X^{\omega}_{jkt},\ H^{\omega}_{bjt},\ W^{\omega}_{bjt} \geqslant 0 \quad \forall b \in \mathscr{B},\ i \in \mathscr{I},\ j \in \mathscr{J},\ k \in \mathscr{K},\ t \in \mathscr{T},\ \omega \in \Omega \quad (11)$$

In **[DP]**, the object of the model is to minimize both the cost of the first-stage and the expected value of the random second-stage. The first term of the objective function minimizes the total set-up cost of establishing the depots. The second term represents the cost of routing feedstock from supply sites to depots along with procurement cost of feedstock at the supplier sites. The third term represents the cost of routing feedstock from depots to markets along with pellet production cost at depot locations. The fourth term of the objective function represents the cost of storing

densified feedstock in the supply chain network. The last term of the objective function is the penalty cost for feedstock demand shortage.

Constraints (2) limit the availability of feedstock supply of type $b \in \mathscr{B}$ at site $i \in \mathscr{I}$ in time period $t \in \mathscr{T}$ and under scenario $\omega \in \Omega$. Constraints (3) enforce flow-conservation at depot pellet processing site $j \in \mathscr{J}$. Constraints (4) limit the amount of feedstock that can be stored in a depot pellet processing site $j \in \mathscr{J}$. Constraints (5) limit the amount of densified feedstock that can be produced in a depot pellet processing site $j \in \mathscr{J}$. Constraints (6) indicate that the amount of feedstock processed in depot pellet processing site $j \in \mathscr{J}$ is limited by the facility capacity c^s_{lmj}. Constraints (7) indicate that the amount of feedstock shipped in market $k \in \mathscr{K}$ is limited by the facility capacity c^p_{lmj}. Constraints (8) indicate that the demand for feedstock must be satisfied either through the supply chain network or through the substitute product. Constraints (9) ensure that at most one depot pellet processing site of capacity $l \in \mathscr{L}$ is operating at a particular location $j \in \mathscr{J}$. Finally, constraints (10) are the binary constraints and (11) are the standard non-negativity constraints.

Although the key objective for model **[DP]** is to minimize cost, with the increase in greenhouse gas (GHG) emissions, it is also imperative for decision makers to reduce CO_2 emissions from the supply chain network. To have a more viable model **[DP]** is extended to **[EDP]** where we introduce a carbon trading mechanism that allows the decision makers to sell or buy carbon credits while monitoring emissions from the supply chain network. We denote CO^{ω}_{2t} as amount of carbon dioxide (CO_2) that is currently emitted (in tons) at time period $t \in \mathscr{T}$ under scenario $\omega \in \Omega$. Let, e^1_{bijt} denote emissions due to per unit feedstock of type $b \in \mathscr{B}$ transporting from supply site $i \in \mathscr{I}$ to depot in location $j \in \mathscr{J}$ at time period $t \in \mathscr{T}$; e^2_{bjt} denotes emissions due to per unit of densified feedstock of type $b \in \mathscr{B}$ stored in location $j \in \mathscr{J}$ at time period $t \in \mathscr{T}$; e^3_{jkt} denotes emissions due to per unit densified biomass transporting from depot in location $j \in \mathscr{J}$ to market $k \in \mathscr{K}$ at time period $t \in \mathscr{T}$; and, $\overline{CO_{2t}}$ denotes the maximum amount (in tons) of carbon dioxide (CO_2) that can be emitted per allotment by the government. The MILP formulation **[EDP]** for the supply chain network can be stated as follows:

$$
\begin{aligned}
[\mathbf{EDP}]\ \underset{\mathbf{Y},\mathbf{X},\mathbf{H},\mathbf{W},\mathbf{U}}{Minimize}\ & \sum_{l\in\mathscr{L}}\sum_{m\in\mathscr{M}}\sum_{j\in\mathscr{J}}\psi_{lmj}Y_{lmj} \\
& + \sum_{t\in\mathscr{T}}\sum_{\omega\in\Omega}\rho_{\omega}\left(\sum_{b\in\mathscr{B}}\sum_{i\in\mathscr{I}}\sum_{j\in\mathscr{J}}(c_{bijt}+\sigma_{bit})X^{\omega}_{bijt} + \sum_{j\in\mathscr{J}}\sum_{k\in\mathscr{K}}(c_{jkt}+p_{jt})X^{\omega}_{jkt}\right. \\
& \left. +\gamma\left(CO^{\omega}_{2t}-\overline{CO_{2t}}\right) + \sum_{b\in\mathscr{B}}\sum_{j\in\mathscr{J}}h_{jt}H^{\omega}_{bjt} + \sum_{k\in\mathscr{K}}\pi_{kt}U^{\omega}_{kt}\right) \qquad (12)
\end{aligned}
$$

Subject to (2)–(11), and

$$
\sum_{b\in\mathscr{B}}\sum_{i\in\mathscr{I}}\sum_{j\in\mathscr{J}}e^1_{bijt}X^{\omega}_{bijt} + \sum_{b\in\mathscr{B}}\sum_{j\in\mathscr{J}}e^2_{bjt}H^{\omega}_{bjt} + \sum_{j\in\mathscr{J}}\sum_{k\in\mathscr{K}}e^3_{jkt}X^{\omega}_{jkt} = CO^{\omega}_{2t}
$$

$$
\forall t \in \mathscr{T},\ \omega \in \Omega \qquad (13)
$$

$$
CO^{\omega}_{2t} \geqslant 0 \quad \forall t \in \mathscr{T},\ \omega \in \Omega \qquad (14)
$$

The current objective function accounts for carbon emissions cost due to carbon trading in addition to investment, production, transportation, procurement,and holding costs as described in model **[DP]**. Constraints (13) calculate the CO_2 emissions across the feedstock supply chain network and constraints (14) are standard non-negativity constraints.

3. Solution approach

In this section, the solution techniques used to solve the **[EDP]** model are discussed. For a single scenario and a single time period i.e., setting $|\Omega| = 1$ and $|\mathscr{T}| = 1$, we can show that the problem **[EDP]]** is actually a special case of an uncapacitated facility location problem known as $\mathscr{NP}$-hard problem. Therefore, commercial solvers such as CPLEX/GUROBI fails to solve any large-scale of such problem (Magnanti & Wong, 1981). To overcome this challenging computational problem, a hybrid sampling based decomposition algorithm that combines Sample Average Approximation method (SAA) with enhanced Progressive Hedging algorithm is proposed. The techniques used to enhance the Progressive Hedging algorithm are local and global adjustment techniques and a rolling horizon algorithm. The aim is to generate high quality feasible solution for problem **[EDP]** in a timely fashion. Details about the hybrid sampling based decomposition algorithm can also be found in Poudel et al. (2016a).

3.1. Sample average approximation

The availability and quantity of feedstock varies from one year to another requiring consideration of large number of scenarios addressing the available feedstock supply in order to develop a two-stage stochastic programming model. However, evaluating large number of scenarios by the model will increase the size of the problem and thus pose significantly computational challenges in solving model **[EDP]**. To remedy this problem, a sampling technique commonly known as the *Sample Average Approximation* (SAA) method is employed to reduce the computational burden in solving model **[EDP]**. SAA is used extensively to solve large scale supply chain network flow related problems, such as Verweij, Ahmed, Kleywegt, Nemhauser, and Shapiro (2003), Santoso et al. (2005), and others. Interested readers may refer to the works of Kleywegt, Shapiro, and Homem-De-Mello (2001) for the proof of convergence properties of SAA and Norkin, Pflug, and Ruszczynski (1998), Norkin, Ermoliev, and Ruszczynski (1998), Shapiro (2005), Mak, Morton, and Wood (1999) for the evaluation of developed statistical inference (validation and error analysis, stopping rules), easily amendable to variance reduction techniques and ideal for parallel computations of SAA. In SAA, a sample $\omega^1, \omega^2, \ldots, \omega^N$ of N realization of the random vector ω is generated from Ω according to a probability distribution $\mathbb{P}$ and they are solved repeatedly until a pre-specified tolerance gap is achieved. After generating the scenarios (e.g., N scenarios), the model **[EDP]**, defined by Eq. (12) subject to constraints (2)–(11), (13) and (14), is approximated by the following SAA problem:

$$
\begin{aligned}
\underset{y\in\mathbf{Y}}{Minimize}\ \Bigg\{ & \hat{g}(Y) := \sum_{l\in\mathscr{L}}\sum_{m\in\mathscr{M}}\sum_{j\in\mathscr{J}}\psi_{lmj}Y_{lmj} \\
& + \sum_{t\in\mathscr{T}}\sum_{n\in\mathscr{N}}\frac{1}{N}\left(\sum_{b\in\mathscr{B}}\sum_{i\in\mathscr{I}}\sum_{j\in\mathscr{J}}(c_{bijt}+\sigma_{bit})X^{n}_{bijt} + \sum_{j\in\mathscr{J}}\sum_{k\in\mathscr{K}}(c_{jkt}+p_{jt})X^{n}_{jkt}\right. \\
& \left. +\gamma\left(CO^{n}_{2t}-\overline{CO_{2t}}\right) + \sum_{b\in\mathscr{B}}\sum_{j\in\mathscr{J}}h_{jt}H^{n}_{bjt} + \sum_{k\in\mathscr{K}}\pi_{kt}U^{n}_{kt}\right)\Bigg\} \qquad (15)
\end{aligned}
$$

As the sample size increases the optimal solution of (15), $\tilde{Y}_N$, and the optimal value v_N, converge with probability one to an optimal solution of the original problem **[EDP]** (Kleywegt et al., 2001). Assuming that the SAA problem is solved within an absolute optimality gap $\delta \geqslant 0$, we can now estimate the sample size N needed to guarantee an ϵ-optimal solution to the problem with probability at least equal to $(1-\alpha)$ as:

$$N \geqslant \frac{3\sigma_{max}^2}{(\epsilon-\delta)^2}(|\mathscr{L}||\mathscr{M}||\mathscr{J}|(\log 2)-\log\alpha) \tag{16}$$

where $\epsilon > \delta$, $\alpha \in (0,1)$ and σ_{max}^2 is a maximal variance of certain function differences (Kleywegt et al., 2001). Sample size estimation using Eq. (16) is too conservative for practical applications. Thus, one can choose a sample size N as a trade-off between the solution quality obtained by solving (15) to the original problem **[EDP]** and the computational burden needed to solve it. In each iteration of the algorithmic step, SAA provides a valid statistical lower and upper bound for the original problem **[EDP]** and the process terminates when the gap between the estimators falls below a pre-specified threshold value. The main steps of the Sample Average Approximation (SAA) approach can be explained as follows.

1. Generate M independent supply scenarios of size N i.e., $\{\mathbf{s}_m^1(\omega),\mathbf{s}_m^2(\omega),\ldots,\mathbf{s}_m^N(\omega)\}$, $\forall m=1,\ldots,M$, where $\mathbf{s}=\{s_{bit}^{\omega}; \forall b\in\mathscr{B},\ i\in\mathscr{I},\ t\in\mathscr{T},\ \omega\in\Omega\}$ and solve the corresponding SAA:

$$\underset{y\in\mathbf{Y}}{Minimize}\Bigg\{\hat{g}(Y):=\sum_{l\in\mathscr{L}}\sum_{m\in\mathscr{M}}\sum_{j\in\mathscr{J}}\psi_{lmj}Y_{lmj} +\sum_{t\in\mathscr{T}}\sum_{n\in\mathscr{N}}\frac{1}{N}\Bigg(\sum_{b\in\mathscr{B}}\sum_{i\in\mathscr{I}}\sum_{j\in\mathscr{J}}(c_{bijt}+\sigma_{bit})X_{bijt}^n+\sum_{j\in\mathscr{J}}\sum_{k\in\mathscr{K}}(c_{jkt}+p_{jt})X_{jkt}^n +\gamma\left(\mathrm{CO}_{2t}^n-\overline{\mathrm{CO}_{2t}}\right)+\sum_{b\in\mathscr{B}}\sum_{j\in\mathscr{J}}h_{jt}H_{bjt}^n+\sum_{k\in\mathscr{K}}\pi_{kt}U_{kt}^n\Bigg)\Bigg\} \tag{17}$$

2. Compute the average of the optimal solutions obtained by solving all SAA problems, $\bar{\mathbf{v}}_M^N$ and variance, $\sigma_{\bar{\mathbf{v}}_M^N}^2$ obtained in **Steps 1** as follows:

$$\bar{\mathbf{v}}_M^N=\frac{1}{M}\sum_{m=1}^{M}\mathbf{v}_N^m$$

$$\sigma_{\bar{\mathbf{v}}_M^N}^2=\frac{1}{(M-1)M}\sum_{m=1}^{M}(\mathbf{v}_N^m-\bar{\mathbf{v}}_M^N)^2$$

The $\bar{\mathbf{v}}_M^N$ is an unbiased estimator of [**EDP**] which is the expected optimal objective function value of the sample problems. Let $v^{\star}$ denote the optimal objective function value of the original problem. Since $\mathbb{E}[v]\leqslant v^{\star}$, the $\bar{\mathbf{v}}_M^N$ provides a statistical lower bound on the optimal objective function value for the original problem.

3. Select a feasible first-stage solution obtained from **Step 1** i.e., one of $\hat{\mathbf{Y}}_N^m$ and solve the original problem using a reference sample N' as follows:

$$\tilde{\mathbf{g}}_{N'}(\widetilde{Y}):=\sum_{l\in\mathscr{L}}\sum_{m\in\mathscr{M}}\sum_{j\in\mathscr{J}}\psi_{lmj}\widetilde{Y_{lmj}}+\sum_{t\in\mathscr{T}}\sum_{n\in\mathscr{N}'}\frac{1}{N'}\Bigg(\sum_{b\in\mathscr{B}}\sum_{i\in\mathscr{I}}\sum_{j\in\mathscr{J}}(c_{bijt}+\sigma_{bit})X_{bijt}^n +\sum_{j\in\mathscr{J}}\sum_{k\in\mathscr{K}}(c_{jkt}+p_{jt})X_{jkt}^n+\gamma\left(\mathrm{CO}_{2t}^n-\overline{\mathrm{CO}_{2t}}\right) +\sum_{b\in\mathscr{B}}\sum_{j\in\mathscr{J}}h_{jt}H_{bjt}^n+\sum_{k\in\mathscr{K}}\pi_{kt}U_{kt}^n\Bigg) \tag{18}$$

The estimator $\tilde{\mathbf{g}}_{N'}(\widetilde{Y})$ serves as an upper bound for the problem **[EDP]** and will be updated in each iteration if the value obtained is less than the value of the previous iteration. We now generate a large set of feedstock supply scenarios $\mathscr{N}'$, i.e., $\{\mathbf{s}^1(\omega),\mathbf{s}^2(\omega),\ldots,\mathbf{s}^{N'}(\omega)\}$, $\forall n=1,\ldots,N'$. Typically, sample size $\mathscr{N}'$ is chosen much larger than the sample size $\mathscr{N}$ in the SAA problems i.e., $N'\gg N$. We can estimate the variance of $\tilde{\mathbf{g}}_{N'}(\widetilde{Y})$ as follows:

$$\sigma_{N'}^2(\widetilde{Y})=\frac{1}{(N'-1)N'}\sum_{n=1}^{N'}\left\{\sum_{l\in\mathscr{L}}\sum_{m\in\mathscr{M}}\sum_{j\in\mathscr{J}}\psi_{lmj}\widetilde{Y}_{lmj}+\sum_{t\in\mathscr{T}}\mathbb{Q}(\mathbf{Y},n))-\tilde{\mathbf{g}}_{N'}(\widetilde{Y})\right\}^2$$

where $\mathbb{Q}(\mathbf{Y},n)$ represents the solution of the second-stage problem.

4. Compute the optimality gap ($gap_{N,M,N'}(\widetilde{Y})$) and its variance ($\sigma_{gap}^2$) using the estimators calculated in **Steps 2** and **3**.

$$gap_{N,M,N'}(\widetilde{Y})=\tilde{\mathbf{g}}_{N'}(\widetilde{Y})-\bar{\mathbf{v}}_M^N$$

$$\sigma_{gap}^2=\sigma_{N'}^2(\widetilde{Y})+\sigma_{\bar{\mathbf{v}}_M^N}^2$$

3.2. Progressive hedging

In **Step1**, the Sample Average Approximation algorithm requires solving a two-stage stochastic programming model of N scenarios. However, the problem is still considered challenging due to the memory and computational time restrictions in solving N scenario subproblems. Often, decomposition based methods are used to divide the problem into smaller and more manageable subproblems (Rockafellar & Wets, 1991), which motivates us to solve each subproblem of the SAA problem using a Progressive Hedging Algorithm (PHA). The PHA proceeds by applying a scenario decomposition technique based on the augmented Lagrangian relaxation scheme to solve a number of individual scenario subproblems and finally aggregate the individual scenario solutions. PHA has proven the first rigorous algorithmic procedure that has been successfully applied to a number of broad application areas such as financial planning (Mulvey & Vladimirou, 1991), surgery planning (Gul, Denton, & Fowler, 2015), and others. Interested readers can review the studies conducted by Wallace and Helgason (1991).

Constraints (4), (6), and (7) in [**EDP**] link the first-stage decisions with the second-stage decision variables. These constraints do not allow problem (17) to be separable by scenarios. To remedy this problem, we create a copy of $\{Y_{lmj}^n\}_{\forall l\in\mathscr{L},m\in\mathscr{M},j\in\mathscr{J},n\in\mathscr{N}}\in\{0,1\}$, of the first-stage variables for each scenario $n\in\mathscr{N}$. Problem (17) can now be rewritten as follows:

$$\underset{\mathbf{Y},\mathbf{X},\mathbf{H},\mathbf{W},\mathbf{U}}{Minimize}\ \frac{1}{N}\sum_{n\in\mathscr{N}}\Bigg(\sum_{l\in\mathscr{L}}\sum_{m\in\mathscr{M}}\sum_{j\in\mathscr{J}}\psi_{lmj}Y_{lmj}^n+\sum_{t\in\mathscr{T}}\Bigg(\sum_{b\in\mathscr{B}}\sum_{i\in\mathscr{I}}\sum_{j\in\mathscr{J}}(c_{bijt}+\sigma_{bit})X_{bijt}^n +\sum_{j\in\mathscr{J}}\sum_{k\in\mathscr{K}}(c_{jkt}+p_{jt})X_{jkt}^n+\gamma\left(\mathrm{CO}_{2t}^{\omega}-\overline{\mathrm{CO}_{2t}}\right)+\sum_{b\in\mathscr{B}}\sum_{j\in\mathscr{J}}h_{jt}H_{bjt}^n+\sum_{k\in\mathscr{K}}\pi_{kt}U_{kt}^n\Bigg)\Bigg) \tag{19}$$

Subject to (2), (3), (5), (8), (11), (13), (14), and

$$\sum_{b\in\mathscr{B}}H_{bjt}^n\leqslant\sum_{l\in\mathscr{L}}h_{lmj}^{cap}Y_{lmj}^n\quad\forall m\in\mathscr{M},\ j\in\mathscr{J},\ t\in\mathscr{T},\ n\in\mathscr{N} \tag{20}$$

$$\sum_{b\in\mathscr{B}}W_{bjt}^n\leqslant\sum_{l\in\mathscr{L}}c_{lmj}^sY_{lmj}^n\quad\forall m\in\mathscr{M},\ j\in\mathscr{J},\ t\in\mathscr{T},\ n\in\mathscr{N} \tag{21}$$

$$\sum_{k\in\mathscr{K}}X_{jkt}^n\leqslant\sum_{l\in\mathscr{L}}c_{lmj}^pY_{lmj}^n\quad\forall m\in\mathscr{M},\ j\in\mathscr{J},\ t\in\mathscr{T},\ n\in\mathscr{N} \tag{22}$$

$$Y_{lmj}^n=Y_{lmj}^v\quad\forall n,\ v\in\mathscr{N},\ n\neq v \tag{23}$$

$$Y_{lmj}^n\in\{0,1\}\quad\forall l\in\mathscr{L},\ m\in\mathscr{M},\ j\in\mathscr{J},\ n\in\mathscr{N} \tag{24}$$

Constraints (23) are referred to as *nonanticipativity* constraints which link the first and second-stage decision variables and force all the scenarios to yield the same first-stage decision variable making the model not separable by scenarios. To make the model separable by scenarios and apply Lagrangian relaxation, we need to rewrite the *nonanticipativity* constraints. Letting $\{\overline{Y}_{lmj}\}_{\forall l\in\mathscr{L},m\in\mathscr{M}j\in\mathscr{J}}\in\{0,1\}$ be the "overall design vector"; the following constraints are equivalent to (23):

$$Y_{lmj}^n=\overline{Y}_{lmj}\quad\forall l\in\mathscr{L},\ m\in\mathscr{M},\ j\in\mathscr{J},\ n\in\mathscr{N} \tag{25}$$

$$\overline{Y}_{lmj}\in\{0,1\}\quad\forall l\in\mathscr{L},\ m\in\mathscr{M},\ j\in\mathscr{J} \tag{26}$$

Following the decomposition technique proposed by Rockafellar and Wets (1991), we relax constraints (25) using an augmented Lagrangian strategy and obtain the following objective function:

$$\underset{\mathbf{Y},\mathbf{X},\mathbf{H},\mathbf{W},\mathbf{U}}{Minimize}\ \frac{1}{N}\sum_{n\in\mathcal{N}}\Bigg(\sum_{l\in\mathcal{L}}\sum_{m\in\mathcal{M}}\sum_{j\in\mathcal{J}}\psi_{lmj}Y^n_{lmj}+\sum_{t\in\mathcal{T}}\Bigg(\sum_{b\in\mathcal{B}}\sum_{i\in\mathcal{I}}\sum_{j\in\mathcal{J}}(c_{bijt}+\sigma_{bit})X^n_{bijt}$$
$$+\sum_{j\in\mathcal{J}}\sum_{k\in\mathcal{K}}(c_{jkt}+p_{jt})X^n_{jkt}+\gamma\left(CO^{\omega}_{2t}-\overline{CO_{2t}}\right)+\sum_{b\in\mathcal{B}}\sum_{j\in\mathcal{J}}h_{jt}H^n_{bjt}+\sum_{k\in\mathcal{K}}\pi_{kt}U^n_{kt}\Bigg)$$
$$+\lambda^n_{lmj}(Y^n_{lmj}-\overline{Y}_{lmj})+\frac{1}{2}\sigma(Y^n_{lmj}-\overline{Y}_{lmj})^2\Bigg) \tag{27}$$

where $\{\lambda^n_{lmj}\}_{\forall l\in\mathcal{L},m\in\mathcal{M}\,j\in\mathcal{J},n\in\mathcal{N}}$, defines the Lagrangian multipliers for the relaxed constraints and σ defines the penalty ratio. Given the binary requirement of the design variables, $\{Y^n_{lmj}\}_{\forall l\in\mathcal{L},m\in\mathcal{M},j\in\mathcal{J},n\in\mathcal{N}}$ and $\{\overline{Y}_{lmj}\}_{\forall l\in\mathcal{L},m\in\mathcal{M}\,j\in\mathcal{J}}$ the quadratic term $\sum_{l\in\mathcal{L},m\in\mathcal{M},j\in\mathcal{J}}\sigma(Y^n_{lmj}-\overline{Y}_{lmj})^2$ shown in the objective function can be reduced as follows:

$$\sum_{l\in\mathcal{L}}\sum_{m\in\mathcal{M}}\sum_{j\in\mathcal{J}}\sigma(Y^n_{lmj}-\overline{Y}_{lmj})^2=\sum_{l\in\mathcal{L}}\sum_{m\in\mathcal{M}}\sum_{j\in\mathcal{J}}\left(\sigma(Y^n_{lmj})^2-2Y^n_{lmj}\overline{Y}_{lmj}+\sigma(\overline{Y}_{lmj})^2\right)$$
$$=\sum_{l\in\mathcal{L}}\sum_{m\in\mathcal{M}}\sum_{j\in\mathcal{J}}\left(\sigma Y^n_{lmj}-2\sigma Y^n_{lmj}\overline{Y}_{lmj}+\sigma\overline{Y}_{lmj}\right)$$

Then the objective function can be reduced as follows

$$\underset{\mathbf{Y},\mathbf{X},\mathbf{H},\mathbf{W},\mathbf{U}}{Minimize}\ \frac{1}{N}\sum_{n\in\mathcal{N}}\Bigg(\sum_{l\in\mathcal{L}}\sum_{m\in\mathcal{M}}\sum_{j\in\mathcal{J}}\left(\psi_{lmj}+\lambda^n_{lmj}-\sigma\overline{Y}_{lmj}+\frac{\sigma}{2}\right)Y^n_{lmj}$$
$$++\sum_{t\in\mathcal{T}}\Bigg(\sum_{b\in\mathcal{B}}\sum_{i\in\mathcal{I}}\sum_{j\in\mathcal{J}}(c_{bijt}+\sigma_{bit})X^n_{bijt}+\sum_{j\in\mathcal{J}}\sum_{k\in\mathcal{K}}(c_{jkt}+p_{jt})X^n_{jkt}$$
$$+\gamma\left(CO^{\omega}_{2t}-\overline{CO_{2t}}\right)+\sum_{b\in\mathcal{B}}\sum_{j\in\mathcal{J}}h_{jt}H^n_{bjt}+\sum_{k\in\mathcal{K}}\pi_{kt}U^n_{kt}\Bigg)+\lambda^n_{lmj}\overline{Y}_{lmj}+\frac{1}{2}\sigma\overline{Y}_{lmj}\Bigg) \tag{28}$$

The last two terms of the objective function become constant for a given overall design $\{\overline{Y}_{lmj}\}_{\forall l\in\mathcal{L},m\in\mathcal{M}\,j\in\mathcal{J}}$. This allows the sub-problems to be decomposable by scenarios $n\in\mathcal{N}$, and the overall problem can be formulated as follows:

$$[\mathbf{EDP(PHA)}]\ \underset{\mathbf{Y},\mathbf{X},\mathbf{H},\mathbf{W},\mathbf{U}}{Minimize}\ \frac{1}{N}\sum_{n\in\mathcal{N}}\Bigg(\sum_{l\in\mathcal{L}}\sum_{m\in\mathcal{M}}\sum_{j\in\mathcal{J}}\left(\psi_{lmj}+\lambda^n_{lmj}-\sigma\overline{Y}_{lmj}+\frac{\sigma}{2}\right)Y^n_{lmj}$$
$$+\sum_{t\in\mathcal{T}}\Bigg(\sum_{b\in\mathcal{B}}\sum_{i\in\mathcal{I}}\sum_{j\in\mathcal{J}}(c_{bijt}+\sigma_{bit})X^n_{bijt}+\sum_{j\in\mathcal{J}}\sum_{k\in\mathcal{K}}(c_{jkt}+p_{jt})X^n_{jkt}$$
$$+\gamma\left(CO^{\omega}_{2t}-\overline{CO_{2t}}\right)+\sum_{b\in\mathcal{B}}\sum_{j\in\mathcal{J}}h_{jt}H^n_{bjt}+\sum_{k\in\mathcal{K}}\pi_{kt}U^n_{kt}\Bigg)\Bigg) \tag{29}$$

Subject to

$$\sum_{j\in\mathcal{J}}X^n_{bijt}\leqslant s^n_{bit}\quad\forall b\in\mathcal{B},\ i\in\mathcal{I},\ t\in\mathcal{T} \tag{30}$$
$$\sum_{i\in\mathcal{I}}X^n_{bijt}+(1-\alpha_b)H^n_{bjt-1}=H^n_{bjt}+W^n_{bjt}\quad\forall b\in\mathcal{B},\ j\in\mathcal{J},\ t\in\mathcal{T} \tag{31}$$
$$\sum_{b\in\mathcal{B}}H^n_{bjt}\leqslant\sum_{l\in\mathcal{L}}h^{cap}_{lmj}Y^n_{lmj}\quad\forall m\in\mathcal{M},\ j\in\mathcal{J},\ t\in\mathcal{T} \tag{32}$$
$$\sum_{k\in\mathcal{K}}X^n_{jkt}\leqslant\sum_{b\in\mathcal{B}}\phi_bW^n_{bjt}\quad\forall j\in\mathcal{J},\ t\in\mathcal{T} \tag{33}$$
$$\sum_{b\in\mathcal{B}}W^n_{bjt}\leqslant\sum_{l\in\mathcal{L}}c^s_{lmj}Y^n_{lmj}\quad\forall m\in\mathcal{M},\ j\in\mathcal{J},\ t\in\mathcal{T} \tag{34}$$
$$\sum_{k\in\mathcal{K}}X^n_{jkt}\leqslant\sum_{l\in\mathcal{L}}c^p_{lmj}Y^n_{lmj}\quad\forall m\in\mathcal{M},\ j\in\mathcal{J},\ t\in\mathcal{T} \tag{35}$$
$$\sum_{j\in\mathcal{J}}X^n_{jkt}+U^n_{kt}=d_{kt}\quad\forall k\in\mathcal{K},\ t\in\mathcal{T} \tag{36}$$
$$\sum_{b\in\mathcal{B}}\sum_{i\in\mathcal{I}}\sum_{j\in\mathcal{J}}e^1_{bijt}X^n_{bijt}+\sum_{b\in\mathcal{B}}\sum_{j\in\mathcal{J}}e^2_{bjt}H^n_{bjt}+\sum_{j\in\mathcal{J}}\sum_{k\in\mathcal{K}}e^3_{jkt}X^n_{jkt}=CO^n_{2t}\quad\forall t\in\mathcal{T} \tag{37}$$
$$\sum_{l\in\mathcal{L}}\sum_{m\in\mathcal{M}}Y^n_{lmj}\leqslant 1\quad\forall j\in\mathcal{J} \tag{38}$$
$$Y^n_{lmj}\in\{0,1\}\quad\forall l\in\mathcal{L},\ m\in\mathcal{M},\ j\in\mathcal{J} \tag{39}$$
$$X^n_{bijt},X^n_{jkt},H^n_{bjt},W^n_{bjt},CO^n_{2t}\geqslant 0\quad\forall b\in\mathcal{B},\ i\in\mathcal{I},\ j\in\mathcal{J},\ k\in\mathcal{K},\ t\in\mathcal{T} \tag{40}$$

Here, $\{\lambda^{n,r}_{lmj}\}_{\forall l\in\mathcal{L},m\in\mathcal{M}\,j\in\mathcal{J},n\in\mathcal{N}}$ and σ^r denote the Lagrangian multipliers and penalty parameter of the progressive hedging algorithm, respectively which are updated at each iteration r. The general idea of the basic Progressive hedging algorithm is to solve N deterministic **[EDP(PHA)]** problem and obtain the consensus parameter $\{\overline{Y}^r_{lmj}\}_{\forall l\in\mathcal{L},m\in\mathcal{M}\,j\in\mathcal{J}}$. If the gap between the binary variable $Y^{n,r}_{lmj}$ and the consensus parameter $\overline{Y}^r_{lmj}$ falls below a threshold value ϵ (i.e., $\epsilon=0.001$) for each $l\in\mathcal{L},m\in\mathcal{M},j\in\mathcal{J}$ then the algorithm terminates; otherwise, the value of $\lambda^{n,r}_{lmj}$ and σ^r are updated using Eqs. (41) and (42) and the process continues.

$$\lambda^{n,r}_{lmj}\leftarrow\lambda^{n,r-1}_{lmj}+\sigma^{r-1}(Y^{n,r}_{lmj}-\overline{Y}^{r-1}_{lmj})\quad\forall l\in\mathcal{L},\ m\in\mathcal{M},\ j\in\mathcal{J} \tag{41}$$
$$\sigma^r\leftarrow\alpha\sigma^{r-1} \tag{42}$$

where $\alpha>1$ is a given constant and σ^0 is set to a fixed positive value to ensure that $\sigma^r\to\infty$ as the number of iteration r increases. Moreover, $\lambda^{n,0}_{lmj}$ is set to zero for each scenario $n\in\mathcal{N}$. Pseudo-code of the basic progressive hedging algorithm is provided in Algorithm 1.

Algorithm 1. Progressive Hedging Algorithm

Initialize, $r\leftarrow 1,\epsilon,\{\boldsymbol{\lambda}^{n,r}_{lmj}\}_{\forall l\in\mathcal{L},m\in\mathcal{M}\,j\in\mathcal{J},n\in N}\leftarrow 0,\boldsymbol{\sigma}^r\leftarrow\boldsymbol{\sigma}^0$
$\overline{Y}^r_{lmj}\leftarrow 0$
terminate ← **false**
while (*terminate* = **false**) **do**
  for $n=1$ to N
    Solve [**EDP**(**PHA**)] and obtain $\{Y^{n,r}_{lmj}\}_{\forall l\in\mathcal{L},m\in\mathcal{M}\,j\in\mathcal{J},n\in\mathcal{N}}$
  end for
  Calculate the consensus parameter:
    $\overline{Y}^r_{lmj}\leftarrow\frac{1}{N}\sum_{n=1}^{N}Y^{n,r}_{lmj};\forall l\in\mathcal{L},m\in\mathcal{M},j\in\mathcal{J}$
  if $(r>1)$ **then**
    Update the lagrangian parameter:
      $\boldsymbol{\lambda}^{n,r}_{lmj}\leftarrow\boldsymbol{\lambda}^{n,r-1}_{lmj}+\boldsymbol{\sigma}^{r-1}(Y^{n,r}_{lmj}-\overline{Y}^{r-1}_{lmj});$
    $\forall l\in\mathcal{L},m\in\mathcal{M},j\in\mathcal{J}$
    Update the penalty parameter:
      $\boldsymbol{\sigma}^r\leftarrow\alpha\boldsymbol{\sigma}^{r-1}$ and $\alpha>1$
  end if
  if $((Y^{n,r}_{lmj}-\overline{Y}^{r-1}_{lmj})_{\forall l\in\mathcal{L},m\in\mathcal{M},j\in\mathcal{J}}\leqslant\epsilon)$ **then**
    terminate ← **true**
  end if
  $r\leftarrow r+1$
end while

Termination Criteria: The Progressive Hedging algorithm terminates when one of the following condition is satisfied:

- $\frac{1}{N}\sum_{n=1}^{N}\sum_{l\in\mathcal{L},m\in\mathcal{M}\,j\in\mathcal{J},n\in\mathcal{N}}|Y^{n,r}_{lmj}-\overline{Y}^r_{lmj}|\leqslant\epsilon$; where ϵ is a pre-specified tolerance gap
- 10 consecutive non-improvement iterations
- Maximum iteration limit is reached (i.e., $iter^{max}=100$)

- Maximum time limit is reached (i.e., $time^{max}$ = 10,800 CPU seconds)

3.3. Enhancing progressive hedging algorithm

We have observed from the initial computational experimentation that Progressive Hedging algorithm shows faster convergence for small and medium network size problems. However, for a sufficiently large network it takes an extensive amount of time for convergence. This motivates us to explore additional enhancement techniques to improve the convergence and stability of the PHA algorithm. Hence, we explore additional enhancement techniques to solve the problem faster. The following subsection discusses some PHA enhancement techniques that we have investigated in an attempt to make the model [**EDP**(**PHA**)] solve faster.

3.3.1. Penalty parameter updating

Prior studies such as Chen and Fan (2012) and Huang et al. (2014) show that setting the value of σ highly impacts the quality of the solution produced by the Progressive Hedging algorithm. For instance, the algorithm converges faster to a sub-optimal solution for a significantly large value of σ. However, the algorithm takes a longer time to converge if the σ is set to a conservative value. As inspired by Hvattum and Lokketangen (2009), we dynamically adjust the value of $\boldsymbol{\sigma}$ over iterations based on the computational performance obtained from prior iterations of the PHA algorithm. Let Δ_1^r and Δ_2^r define the indicators of the convergence rates in the dual space and in the primal space, respectively, then, the penalty value can be updated as follows:

$$\Delta_1^r = \sum_{l\in\mathscr{L}}\sum_{m\in\mathscr{M}}\sum_{j\in\mathscr{J}}(Y_{lmj}^r - \overline{Y}_{lmj}^r)^2 \tag{43}$$

$$\Delta_2^r = \sum_{l\in\mathscr{L}}\sum_{m\in\mathscr{M}}\sum_{j\in\mathscr{J}}(\overline{Y}_{lmj}^r - \overline{Y}_{lmj}^{r-1})^2 \tag{44}$$

$$\boldsymbol{\sigma}^r = \begin{cases} \theta\boldsymbol{\sigma}^{r-1} & \text{if } \Delta_1^r - \Delta_1^{r-1} > 0 \\ \frac{1}{\theta}\boldsymbol{\sigma}^{r-1} & \text{else if } \Delta_2^r - \Delta_2^{r-1} > 0 \\ \sigma^{r-1} & \text{otherwise} \end{cases} \tag{45}$$

where θ represents a constant parameter, which value is set to $\theta > 1$.

3.3.2. Heuristic strategy

As inspired by Crainic, Fu, Gendreau, Rei, and Wallace (2011), we have used two heuristic strategies that modify the fixed cost of opening depot facilities in problem **[EDP(PHA)]** to further enhance the performance of the Progressive Hedging algorithm. The first strategy, called *global heuristics* modifies the fixed cost of using a depot facility at the end of each iteration. The second strategy, referred to as *local heuristics*, adjusts the fixed cost of opening depot within the scenario level.

Remember that the problem **[EDP(PHA)]** is composed of a series of N deterministic sub-problems. At the end of each iteration r in Algorithm 1, we can obtain the values of the consensus parameter $\{\overline{Y}_{lmj}^r\}_{\forall l\in\mathscr{L},m\in\mathscr{M},j\in\mathscr{J}}$ which provide an indication of how many times a depot facility was opened in the previous iterations. A higher value of $\overline{Y}_{lmj}^r$ signifies that the depot $j \in \mathscr{J}$ of capacity $l \in \mathscr{L}$ of type $m \in \mathscr{M}$ was opened in most of the previous iterations. Conversely, a lower value of $\overline{Y}_{lmj}^r$ indicates that the depot $j \in \mathscr{J}$ of capacity $l \in \mathscr{L}$ of type $m \in \mathscr{M}$ was not a favorable decision in most of the previous iterations. Assume $\overline{c}$ and $\underline{c}$ are the two parameters that define the upper and lower than threshold value. Therefore, if the value of $\overline{Y}_{lmj}^r$ is greater than the threshold value $\overline{c}$, then lowering the fixed cost of opening the depot will motivate the subproblems to use the facility in the coming iterations. Similarly, if the value of $\overline{Y}_{lmj}^r$ is lower than the threshold value $\underline{c}$, then increasing the fixed cost of opening the depot will avoid the subproblems to open the facility in the coming iterations. This will fix the decisions of opening few depot facilities to either one or zero and thus will help to reduce the size of the problem. The adjustment strategy is shown below:

$$\psi_{lmj}^r = \begin{cases} \delta\psi_{lmj}^{r-1} & \text{if } \overline{Y}_{lmj}^{r-1} < \underline{c} \\ \frac{1}{\delta}\psi_{lmj}^{r-1} & \text{if } \overline{Y}_{lmj}^{r-1} > \overline{c} \\ \psi_{lmj}^{r-1} & \text{otherwise} \end{cases} \tag{46}$$

where ψ_{lmj}^r represents the modified fixed cost of opening a depot of capacity $l \in \mathscr{L}$ of type $m \in \mathscr{M}$ in location $j \in \mathscr{J}$ and at iteration r; $\underline{c}$ and $\overline{c}$ are the two constant parameters whose values are set to $0 < \underline{c} < 0.3$ and $0.7 < \overline{c} < 1$; and δ is a constant parameter whose value is set to $\delta > 1$.

The *global heuristics* strategy discussed above can be pushed even further to modify the fixed cost of using depots locally within the scenario level. Crainic et al. (2011) called this the *local heuristics* strategy since the modification of the fixed cost only impacts the subproblem of scenario n at current iteration r. This strategy is emphasized in modifying the fixed cost of opening the depot at scenario $n \in N$ in iteration r if the gap between $Y_{lmj}^{n,r}$ and $\overline{Y}_{lmj}^r$ is sufficiently large. The local adjustment strategy applied to Algorithm 1 is as follows:

$$\psi_{lmj}^{n,r} = \begin{cases} \delta\psi_{lmj}^r & \text{if } |Y_{lmj}^{n,r-1} - \overline{Y}_{lmj}^r| \geqslant c^{far} \text{ and } Y_{lmj}^{n,r-1} = 1 \\ \frac{1}{\delta}\psi_{lmj}^r & \text{if } |Y_{lmj}^{n,r-1} - \overline{Y}_{lmj}^r| \geqslant c^{far} \text{ and } Y_{lmj}^{n,r-1} = 0 \\ \psi_{lmj}^r & \text{otherwise} \end{cases} \tag{47}$$

where $\psi_{lmj}^{n,r}$ represents the modified fixed cost of opening a depot of capacity $l \in \mathscr{L}$ of type $m \in \mathscr{M}$ at location $j \in \mathscr{J}$ under scenario $n \in N$ and at iteration r; c^{far} is a threshold at which point a local adjustment to the fixed cost of opening a depot is applied and is set to $0.5 < c^{far} < 1$; and δ is a constant parameter whose value is set to $\delta > 1$.

3.3.3. Rolling horizon heuristic strategy

The resulting **[EDP(PHA)]** problem is a multi-period deterministic facility location problem. For a large number of time periods, the hybrid algorithm discussed earlier still takes a significant amount of time to solve the problem. This motivates us to explore an additional heuristic approach known as Rolling Horizon **[RH]**. This approach decomposes multi-time period **[EDP(PHA)]** problems into a series of small subproblems with few consecutive time periods and the algorithm terminating when all the subproblems are investigated (Balasubramanian & Grossmann, 2004; Kostina, Guillen-Gosalbeza, Meleb, Bagajewiczc, & Jimeneza, 2011). A pseudo-code of the **[RH]** algorithm is provided in Algorithm 2 that gives readers a better understanding of the working procedure of this heuristic. Let t_0^r define the starting time period of subproblem r and $\mathbf{R}^r$ denote the number of time periods comprised in subproblem r. For each subproblem, we can set a fixed or variable size of $\mathbf{R}^r$ which we initialized to ϑ^r where ϑ^r is a pre-specified step size for each $r \in \mathscr{R}$. The approximating subproblem of the Rolling horizon algorithm is denoted by **[EDP(PHA(r))]**. The approximating subproblems are solved for each scenario $n \in N$ by setting the variables as: (i) $\{Y_{lmj}^n\}_{\forall l\in\mathscr{L},m\in\mathscr{M},j\in\mathscr{J}} \in \{0,1\}$ for $t_0^r \leqslant t \leqslant t_0^r + \mathbf{R}^r$, (ii) $0 \leqslant Y_{lmj}^n \leqslant 1$ for $t > t_0^r + \mathbf{R}^r$. After solving a subproblem, we fix the values of $Y_{lmj}^{n,r} = Y_{lmj}^{n,r-1}$; $\forall l \in \mathscr{L}, m \in \mathscr{M}, j \in \mathscr{J}$ for $t < t_0^r$ and update the step size r. The process continues until all the subproblems are solved. Fig. 5 represents an example of using the rolling horizon approach to solve a problem with three time periods.

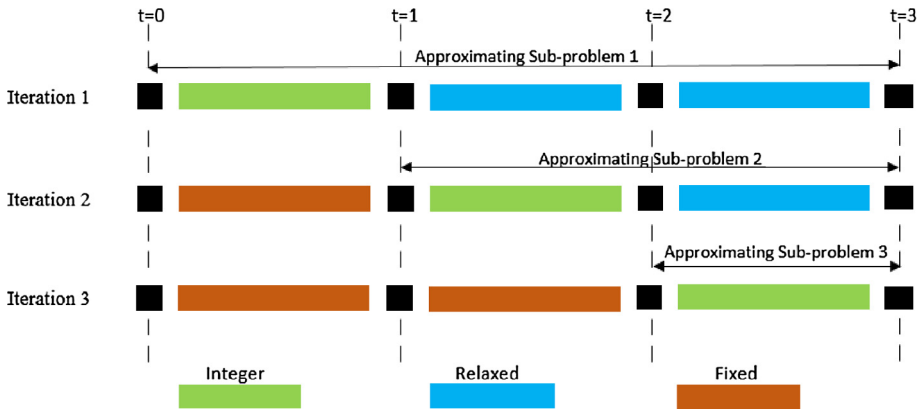

Fig. 5. Illustration of a rolling horizon strategy for a three time period.

4. Computational study and managerial insights

This section conducts numerical studies to test the proposed model **[DP]** and **[EDP]** and draws some managerial insights and recommendations. Mississippi and Alabama have been chosen as a testing case for this study. All the algorithms are coded in GAMS 24.2.1 (General Algebraic Modeling System, 2013) and executed on a desktop computer with Intel Core i7 3.50 GHz processor and 16.0 GB RAM. The optimization solver used is ILOG CPLEX 12.6. The following subsections describe the input parameters used in the study, conduct a computational study on model **[DP]** and **[EDP]**, present results obtained from the case study, draw some managerial insights, and present the performance of the algorithms.

Algorithm 2. Rolling Horizon (RH) Heuristic

$r \leftarrow 1, t_0^r = 0, R^r \leftarrow \vartheta^r$, *terminate* $\leftarrow$ **false**
while (*terminate* = **false**) **do**
  Set:
    $\{Y_{lmj}^n\}_{\forall l \in \mathscr{L}, m \in \mathscr{M}, j \in \mathscr{J}} \in \{0,1\}$ for $t_0^r \leqslant t \leqslant t_0^r + R^r$
    $0 \leqslant \{Y_{lmj}^n\}_{\forall l \in \mathscr{L}, m \in \mathscr{M}, j \in \mathscr{J}} \leqslant 1$ for $t > t_0^r + R^r$
  Solve the approximate sub-problem [**DPHA**] using CPLEX
  if$(t_0 > |\mathscr{T}|)$ **then**
    stop $\leftarrow$ **true**
  else
    Fixing the values of $\{Y_{lmj}^n\}_{\forall l \in \mathscr{L}, m \in \mathscr{M}, j \in \mathscr{J}}$ for $t < t_0^r$
  end if
  $r \leftarrow r + 1$
end while

4.1. Data description

4.1.1. Feedstock supply

Mississippi and Alabama are selected as regions of interest for this research because the three major types of feedstock:forest residue, corn-stove, and miscanthus are readily available in these states. The various feedstocks are highly seasonal and are not necessarily available year round. For instance, while forest residues and miscanthus are available year round except for three months during the winter (December to February), corn-stover is only available from September to November. Mississippi and Alabama produce 3.59 million tons of forest residue, 4.15 million tons of corn-stover, and 1.07 million tons of miscanthus per year (Bioenergy Knowledge Discovery Framework, 2016). In total 180 suppliers from Mississippi and Alabama are considered and their geographic distribution is shown in Fig. 6. The counties that produce fewer than 2500 tons of forest residue, 5000 tons of corn-stover, and 5000 tons of miscanthus are excluded from this study. The average farmgate price of forest residue is set to \$30/dt (Awudu & Zhang, 2013), \$40/dt for corn-stover, and \$40/dt for miscanthus (Bioenergy Knowledge Discovery Framework, 2016).

4.1.2. Feedstock demand

The total annual bio-fuel demand for our test region is set at 225 million gallons per year (MGY) (United States Energy Information Administration, 2015) which will require 3.17 million tons of feedstock to supply. We assume that power plants will replace 6% of coal demand with densified feedstock to produce renewable electricity. This results in a demand of 2.39 million tons per year (MTY) of densified feedstock for the States of Mississippi and Alabama. We further assume that feedstock will fulfill 15% of the demand for total pulp and paper industries and animal feed

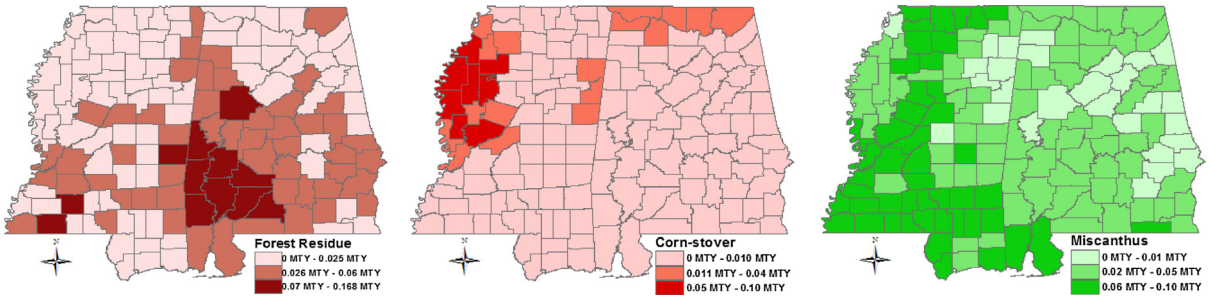

(a) Forest residue (b) Corn-stover (c) Miscanthus

Fig. 6. Geographic distribution of feedstock supplier sites.

markets resulting in a demand of 1.35 million tons and 1.03 million tons on pulp and paper industries and animal feed markets, respectively. We have included a total of 4 bio-refineries, 15 coal-plants, 53 paper-industries, and 38 animal feed markets. Fig. 7 depicts the geographic distribution for all four markets in Mississippi and Alabama.

4.1.3. Total investment cost

Various types of equipment such as grinders, hammer mills, and conveyors are needed to perform the operations in different depots. The equipment prices used in the analysis are collected from local dealers. A total of 60 potential CPP and 123 HMPP and AFEX depot locations are considered. Fig. 8 depicts the location of potential depots in the regions of Mississippi and Alabama. Considering the depot capacity of 0.073 million tons per year (MTY), the total investment costs for CPP and HMPP are about $4.7 million and $3 million, respectively whereas for AFEX it is $8.2 million because the AFEX pre-treatment option requires more operational phases and thus more equipment is needed causing the total investment cost to rise (Lamers et al., 2015). We consider 3 different depot capacities (l = 0.073 MTY, 0.083 MTY, 0.1 MTY). These costs are estimated based on an equipment lifetime of 30 years; a discount factor of 10% is assumed.

4.1.4. Transportation cost

We consider that trucks are used to transport the feedstock from supplier $i \in \mathscr{I}$ to depots $j \in \mathscr{J}$ and from depot $j \in \mathscr{J}$ to market $k \in \mathscr{K}$. The unit cost for truck transportation c_{ij} can be computed as follows (Huang et al., 2010).

$$c_{ij} = \left[\frac{\left(t^d + \frac{t^t}{s_1}\right) d_{ij}}{\delta_1^{cap}} + \Upsilon_1 \right] \quad \forall i \in \mathscr{I},\ j \in \mathscr{J}$$

Here, t^t indicates transportation cost ($/hr/truckload) which is time dependent (for instance capital and labor cost), t^d specifies the transportation cost ($/mile/truckload) which is distance dependent (for example maintenance, fuel and insurance costs). Both costs are different along with traveling distance d_{ij}. On the other hand, loading and unloading costs are fixed and do not depend on traveling costs. All these costs are considered for semi trucks with average traveling speed (s_1) of 40 miles per hour and with a load capacity (δ_1^{cap}) of 25 tons. Table 2 summarizes all the cost parameters (Parker et al., 2008).

4.1.5. Emission data

Emission data due to truck transportation (e^1_{bjit}, e^3_{jkt}) is obtained from GHG Protocol (GHG Protocol, 2015) and is set to 0.297 kg/ton-mile. Emissions due to per unit of densified feedstock stored (e^2_{jt}) in location $j \in \mathscr{J}$ at time period $t \in \mathscr{T}$ for CPP, HMPP, and AFEX is respectively set to 1.55 lb CO2/kWh, 1.70 lb CO_2/kWh, and 1.87 lb CO_2/kWh (US Environmental Protection Agency, 2015). CO_2 emissions were calculated as 21.47 lb/gallon of fuel burned and 0.0155 lb/pound of pellet by considering complete combustion of diesel fuel (US Environmental Protection Agency, 2015). Note that all the units are converted to equivalent ton-unit to use them in Eq. (17).

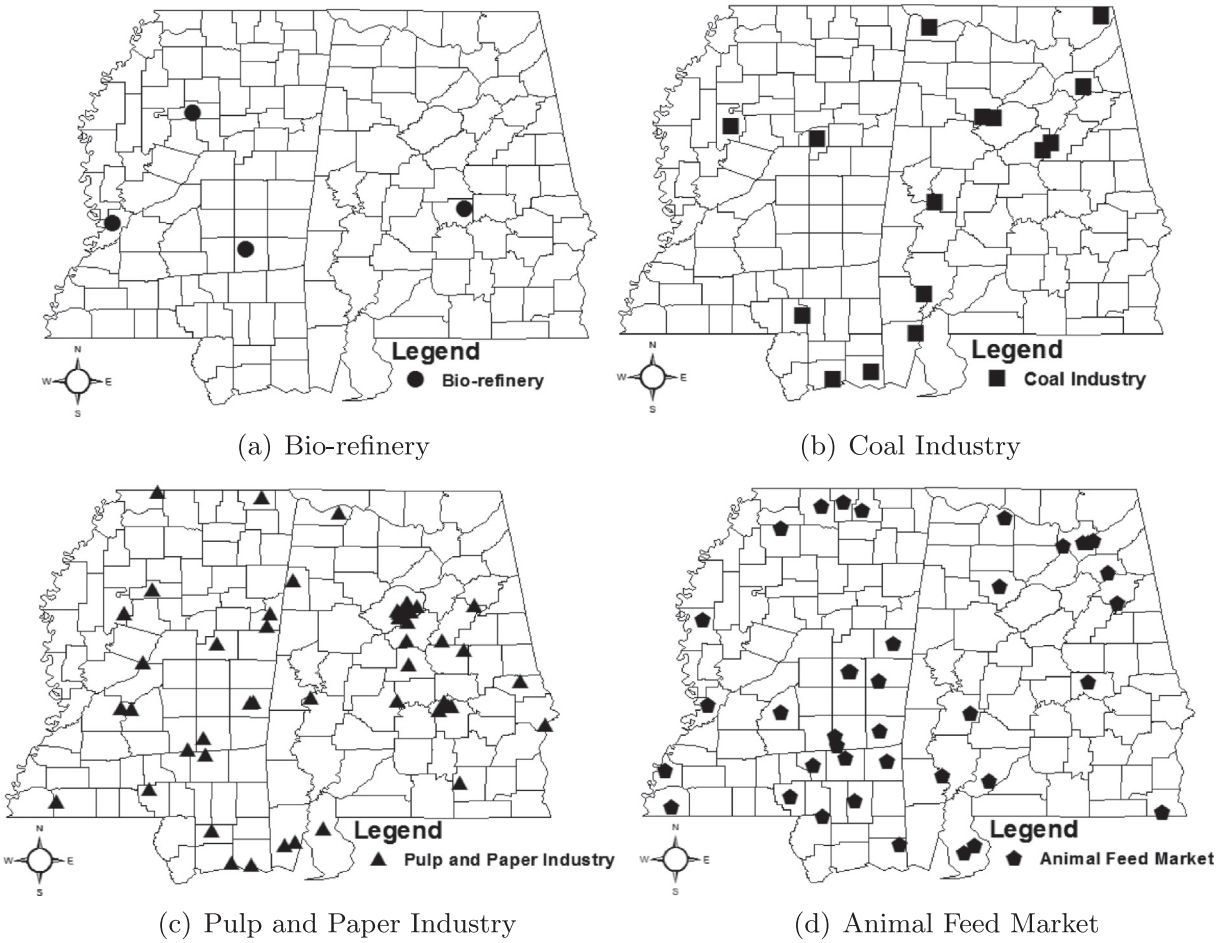

(a) Bio-refinery (b) Coal Industry

(c) Pulp and Paper Industry (d) Animal Feed Market

Fig. 7. Geographic distribution of feedstock demand cities.

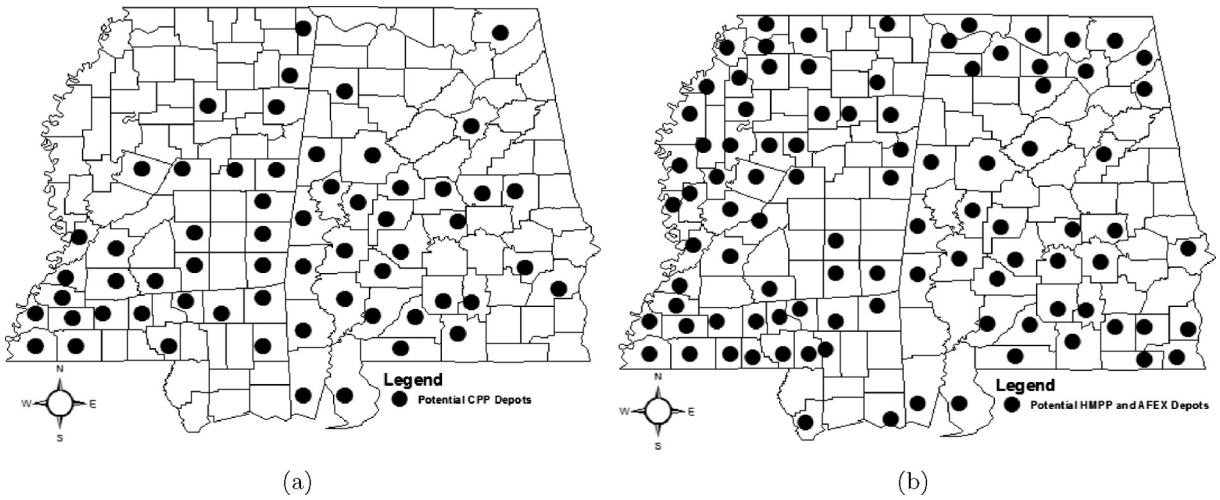

Fig. 8. Potential locations of (a) CPP, (b) HMPP, and AFEX depots.

Table 2
Unit truck transportation cost.

Costs	Parameters	Value	Unit
Loading/unloading	Υ_1	5.0	$/Wet ton
Time dependent	t^t	29.0	$/hr/truck load
Distance dependent	t^d	1.20	$/mile/truck load
Truck capacity	δ_1^{cap}	25	Wet tons

4.2. Analyzing the performance of solution algorithms

In this section the computational experience is analyzed using the proposed solution algorithm introduced in Section 3. For clarification and to facilitate the discussion of our solution approaches, the following notations are introduced:

- **[SAA]**: Sample Average Approximation (SAA) algorithm (described in Section 3.1)
- **[SAA + PHA]**: Hybrid algorithm where the subproblem of the **[SAA]** is solved using Progressive Hedging algorithm (PHA) (described in Section 3.2)
- **[SAA + PHA + HR]**: Hybrid algorithm where the subproblem of the **[SAA]** is solved using an enhanced Progressive Hedging algorithm (PHA) (enhancement techniques described in Sections 3.3.1 and 3.3.2)
- **[SAA + PHA + HR + RH]**: Hybrid algorithm where the subproblem of the **[SAA]** is solved using an enhanced Progressive Hedging algorithm (PHA) (enhancement techniques described in Sections 3.3.1–3.3.3)

The algorithms are terminated when at least one of the following criteria is met: (a) the optimality gap (i.e., $\epsilon = |UB - LB|/UB$) falls below a threshold value $\epsilon = 0.01$; (b) the maximum time limit $time^{max}$ = 10,800 (in CPU seconds) is reached; (c) the maximum number of iterations $iter^{max}$ = 100 is reached. To terminate the Progressive Heading algorithm, some additional stopping criteria have been added and used (as discussed in Section 3.2). The sizes of the deterministic equivalent problems of our model are presented in Table 3. The six problem instances reported in Table 3 are generated by varying the size of $|I|, |J|, |K|$, and $|T|$. The columns of the tables presented in this section (Tables 5 and 6) provide the upper bound, the optimality gap (ϵ), the running time of the algorithms (*in sec*), and the corresponding number of iterations (*Iter*). Table 4 demonstrates the base parameter settings for the initial experimentations.

At this point, we have analyzed the performance of different enhancement techniques which are used to improve the quality of the Progressive Hedging algorithm **[PHA]**. Table 5 shows how the use of different enhancement techniques can speed up the

Table 4
Parameter setting for base case scenario.

Parameters	Symbol	Value
Number of forest residue supply site	$\|I_w\|$	60
Number of corn-stover supply site	$\|I_c\|$	60
Number of miscanthus supply site	$\|I_m\|$	60
Feedstock types	$\|B\|$	3
Number of potential CPP depots	$\|J_w\|$	60
Number of potential HMPP depots	$\|J_c\|$	120
Number of potential AFEX depots	$\|J_m\|$	120
Depot types	$\|M\|$	3
Number of bio-refinery	$\|K_b\|$	4
Number of coal plants	$\|K_c\|$	15
Number of pulp and paper industries	$\|K_p\|$	53
Number of animal feed industries	$\|K_a\|$	38
Number of capacities	$\|L\|$	3
Number of time periods	$\|T\|$	12
Small scenario	N	25
Big scenario	N'	500
Number of replication	Q	5

Table 3
Problem size of the test instances.

Case	$\|I\|$	$\|J\|$	$\|K\|$	$\|L\|$	$\|B\|$	$\|M\|$	$\|T\|$	Binary Variables	Continuous variables	Total variables	No. of constraints
1	60	60	60	3	3	3	4	540	59,524	60,064	121,008
2	60	60	60	3	3	3	8	540	119,048	119,588	241,156
3	60	60	60	3	3	3	12	540	178,572	179,112	361,164
4	180	180	110	3	3	3	4	1620	473,484	475,104	953,268
5	180	180	110	3	3	3	8	1620	946,968	948,588	1,903,116
6	180	180	110	3	3	3	12	1620	1,420,452	1,422,072	2,852,964

Table 5
Performance of enhancement techniques used in PHA.

Case	N	[PHA]				[PHA + HR]				[PHA + HR + RH]			
		UB	GAP (%)	CPU (sec)	Iter	UB	GAP (%)	CPU (sec)	Iter	UB	GAP (%)	CPU (sec)	Iter
1	20	66,620,056	11.25	10,800	21	59,632,173	0.85	1951	7	59,674,303	0.92	**1152**	3
	30	63,788,218	7.31	10,800	34	59,572,090	0.75	2932	6	59,566,089	0.74	**2134**	3
	40	87,385,899	32.34	10,800	24	59,710,462	0.98	4521	12	59,668,281	0.91	**3041**	4
2	20	108,598,375	9.26	10,800	15	99,457,172	0.92	3642	9	99,286,817	0.75	**2454**	5
	30	114,238,541	13.74	10,800	37	99,507,387	0.97	4675	8	99,206,852	0.67	**3242**	2
	40	125,739,653	21.63	10,800	41	99,517,437	0.98	6985	12	99,246,818	0.71	**4231**	3
3	20	265,698,247	7.28	10,800	24	248,317,120	0.79	4625	8	248,367,189	0.81	**3641**	4
	30	269,594,457	8.62	10,800	21	248,492,450	0.86	8652	13	248,292,093	0.78	**5524**	5
	40	330,190,879	25.39	10,800	19	248,567,667	0.89	9642	12	248,642,929	0.92	**7642**	4
4	20	839,445,450	10.15	10,800	27	761,475,757	0.95	8512	8	760,400,985	0.81	**5451**	2
	30	860,515,387	12.35	10,800	38	760,707,753	0.85	**6023**	8	760,554,338	0.83	7541	3
	40	938,929,089	19.67	10,800	34	761,475,757	0.95	10,534	11	760,784,484	0.86	**9642**	3
5	20	954,637,287	8.13	10,800	26	885,168,829	0.92	9658	8	885,079,499	0.91	**7651**	4
	30	978,276,939	10.35	10,800	21	902,753,758	2.85	10,800	8	884,008,946	0.79	**9642**	5
	40	1,302,577,270	32.67	10,800	24	916,623,407	4.32	10,800	7	887,767,259	**1.21**	10,800	4
6	20	1,139,742,838	13.54	10,800	21	1,056,299,344	6.71	10,800	9	994,571,718	0.92	**9634**	6
	30	1,124,268,863	12.35	10,800	13	1,114,982,641	11.62	10,800	13	994,170,357	0.88	**10,432**	5
	40	1,533,014,403	35.72	10,800	21	1,126,067,487	12.49	10,800	16	1,008,000,878	**2.24**	10,800	6
Average		616,847,881	16.21	10,800	25.6	528,240,483	2.76	7779	9.7	508,738,324	**0.93**	**6370**	3.9

convergence and improve the quality of the **[PHA]** algorithm. The enhancement techniques used are: (i) **[PHA + HR]** which incorporates heuristics strategies (described in Section 3.3.2) and penalty parameter updating techniques (described in Section 3.3.1) in **[PHA]** algorithm and (ii) **[PHA + HR + RH]** which incorporates rolling horizon algorithm (described in Section 3.3.3) with heuristics strategies (described in Section 3.3.2), and penalty parameter updating techniques (described in Section 3.3.1) in **[PHA]** algorithm. We consider six cases and three scenario sizes $N = \{20, 30, 40\}$ to obtain 18 different problem instances.

It can be noted that, the experiments run with CPLEX deplete available memory in solving all the problem instances described in Table 5. In any of the experimental results, if the algorithms are solved in less than the stopping criteria ϵ then the algorithm with the smallest running time is highlighted. Otherwise, if such a quality solution is not obtained within the maximum time or iteration limit then the algorithm with the smallest optimality gap is highlighted. It is observed from the results that algorithm **[PHA + HR]** solves 13 out of 18 problem instances, whereas the standard Progressive hedging algorithm **[PHA]** fails to solve any problem instances by obeying the termination criteria. Results indicate that the performance of the algorithm **[PHA + HR]** can be enhanced even further by incorporating rolling horizon framework **[PHA + HR + RH]**. It is observed that algorithm **[PHA + HR + RH]** outperformed **[PHA + HR]** by solving 16 out of 18 problem instances by obeying termination criteria. The overall average optimality gap for algorithm **[PHA + HR + RH]** is 0.93% which is achieved 1.22 times faster than algorithm **[PHA + HR]**. We found that although algorithm **[PHA + HR + RH]** terminates with an ϵ-optimal solution, the quality of solution produced by the **[PHA + HR + RH]** algorithm is consistently high (see Table 5).

We further analyze the performance of the proposed algorithms using problem instances described in Table 3. In Table 6, we present the results from solving the model using the algorithms proposed in Section 3. The problems were solved using *Cases 5 and 6* problem instances obtained from Table 3 with varying sample size N and replication number Q in the **[SAA]** algorithm. We set the large scenario $N' = 500$ to evaluate the SAA gap. In this table, we do not present results obtained from CPLEX because CPLEX deplete available memory in solving all the problem instances reported in Table 6. Results indicate that, **[SAA]** is able to solve only 2 out of 12 problem instances by obeying the termination criteria. The performance can

Table 6
Comparison of different solution approaches.

Case	N	Q	**[SAA]**			**[SAA + PH]**			**[SAA + PHA + HR]**			**[SAA + PHA + HR + RH]**		
			GAP (%)	CPU (sec)	Iter	GAP (%)	CPU (sec)	Iter	GAP (%)	CPU (sec)	Iter	GAP (%)	CPU (sec)	Iter
5	20	5	0.76	8564	1	0.65	7864	2	0.56	5942	2	0.79	**4821**	2
		10	6.56	10,800	1	0.73	9754	4	0.67	6874	1	0.89	**5861**	1
	30	5	8.96	10,800	1	5.42	10,800	2	0.76	8971	2	0.92	5442	1
		10	OOM[a]	–	–	OOM	–	–	3.67	10,800	1	0.81	**7996**	2
	40	5	OOM	–	–	OOM	–	–	0.84	**7153**	1	0.87	7535	1
		10	OOM	–	–	OOM	–	–	4.74	10,800	1	0.94	**8654**	2
6	20	5	0.85	9586	1	0.75	8649	2	0.86	7214	1	0.91	**6421**	1
		10	OOM	–	–	0.69	10,362	1	0.87	8965	1	0.76	**7825**	1
	30	5	OOM	–	–	4.39	10,800	1	0.68	10,354	2	0.96	**7241**	2
		10	OOM	–	–	OOM	–	–	4.25	10,800	1	0.87	**8694**	1
	40	5	OOM	–	–	OOM	–	–	5.29	10,800	1	0.91	**10,364**	1
		10	OOM	–	–	OOM	–	–	6.86	10,800	1	**1.39**	10,800	2
Average			4.28[b]	9937.5	1.0	2.11[b]	9704.8	1.5	2.50	9181.1	1.4	**0.94**	**7637.5**	1.4

[a] Out of Memory.
[b] Instances with (a) did not contribute to average calculation.

be improved slightly by solving the subproblems of the **[SAA]** algorithm using **[PHA]** algorithm. It is observed that algorithm **[SAA + PHA]** is now able to solve 4 out of 12 problem instances by obeying termination criteria. The benefits of using the algorithms become much more evident when the enhancement techniques (developed in Section 3.3) implemented in **[PHA]** algorithm are used to solve the subproblems of the **[SAA]** algorithm. The overall average optimality gap for the **[SAA + PHA + HR]** algorithm is reported as 2.50%, with 7 out of 12 problem instances being solved by obeying termination criteria. On the other hand, the overall average optimality gap for the **[SAA + PHA + HR + RH]** algorithm is reported as 0.94%, with 11 out of 12 problem instances solved in a less than 1.0% optimality gap within the specified time limit. It is important to note that algorithm **[SAA + PHA + HR + RH]** saves 16.81% time over algorithm **[SAA + PHA + HR]**. In summary, the **[SAA + PHA + HR + RH]** algorithm seems to offer consistently high quality solutions within the experimental range.

4.3. Experimental results

4.3.1. Impact of feedstock supply variation levels on system performance

The first set of experiments shows how different levels of supply variation impact the feedstock supply chain network performance. We have generated scenarios using Monte Carlo simulation in which the supply for each period is independent and varies in the range $[\bar{s}_{bit}(1-\epsilon), \bar{s}_{bit}(1+\epsilon)]$ for each feedstock type $b \in \mathscr{B}$ in location $i \in \mathscr{I}$ and at time period $t \in \mathscr{T}$. Note that $\bar{s}_{bit}$ represents the mean feedstock supply scenario for each feedstock type $b \in \mathscr{B}$ in location $i \in \mathscr{I}$ and at time period $t \in \mathscr{T}$ and we assume that the feedstock supply follows uniform distribution. We create two realistic scenarios where we set $\epsilon = 50\%$ and $\epsilon = 5\%$ to represent high and low supply variation levels, respectively. Fig. 9 presents the impact of different feedstock supply variation levels on supply chain network performance. In the experiment, we set $t = 1$ as the month of June. Results indicate that as the level of feedstock supply variability increases the amount of feedstock transporting between the links $(j,k) \in \mathscr{A}_2$ in each time period $t \in \mathscr{T}$ would increase as well. We also observe that to cope with high feedstock supply variability levels, the depots tend to store more feedstock during the off production seasons (December to February) when no feedstock is available. This in turn decreases the overall shortage quantity of feedstock supply in depot $k \in \mathscr{K}$ at time period $t \in \mathscr{T}$.

Fig. 10 shows the distribution of depot facilities under low and high feedstock supply variability levels. Results indicate that as the level of feedstock supply variation increases, the number of depot facilities also increases. More specifically, the model decides to use four additional depot facilities to cope with high feedstock variability. It is important to note that the facilities are now distributing their capacities to minimize the overall transportation costs. For example, in low feedstock variations the model decides to use: three CPP depots of capacities 0.073 MTY, 0.083 MTY, and 0.1 MTY; two HMPP depots of capacities 0.083 MTY, and 0.1 MTY; and three AFEX depots of capacities 0.083 MTY, and 0.1 MTY. However, as the level of variation increases the model decides to use: four CPP depots of capacities 0.073 MTY, 0.083 MTY, and 0.1 MTY; four HMPP depots of capacities 0.073 MTY, 0.083 MTY, and

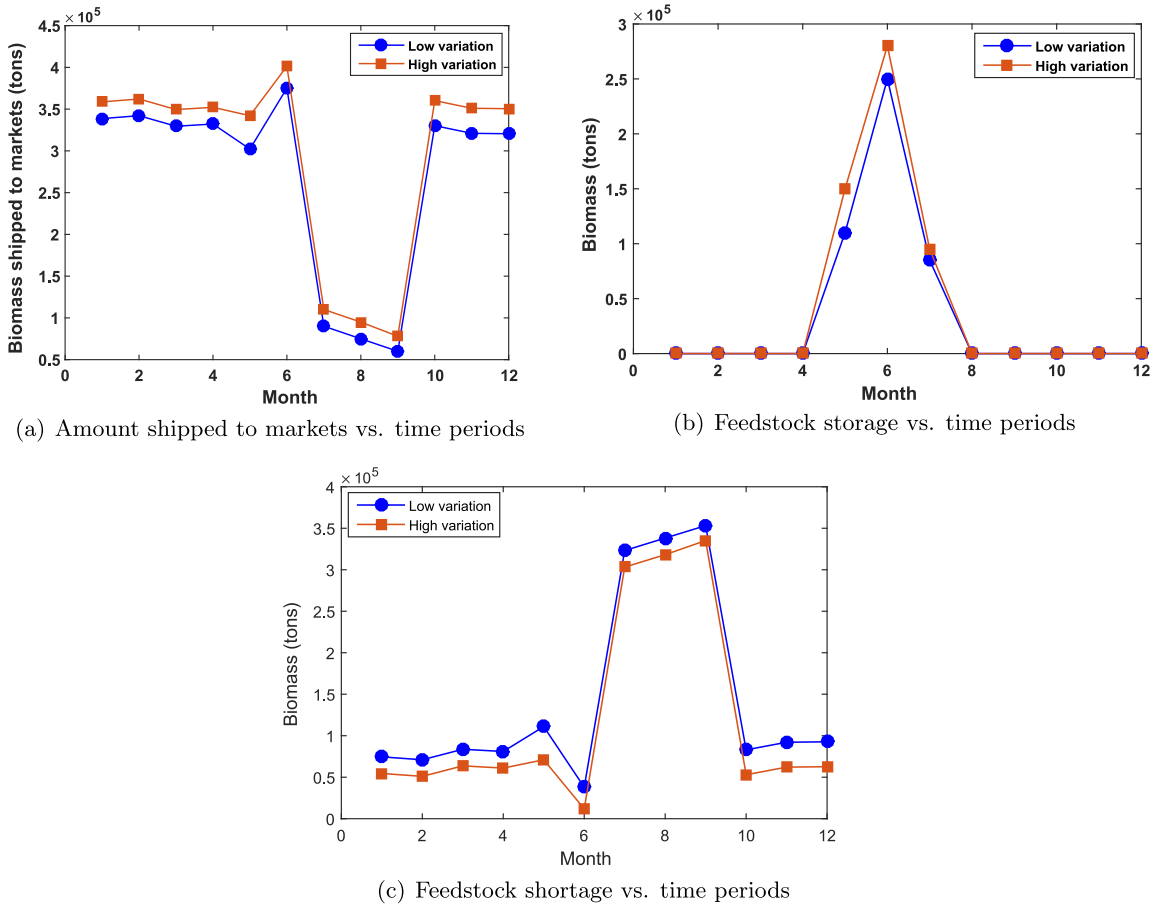

(a) Amount shipped to markets vs. time periods

(b) Feedstock storage vs. time periods

(c) Feedstock shortage vs. time periods

Fig. 9. Supply chain network decisions under different feedstock supply variability levels.

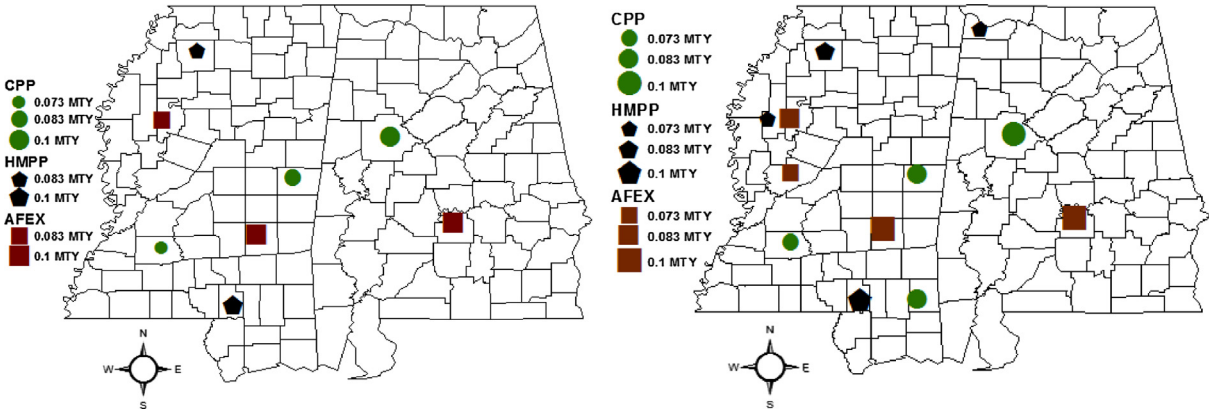

(a) Low supply variability (b) High supply variability

Fig. 10. Impact of feedstock supply variability on network configuration.

0.1 MTY; and four AFEX depots of capacities 0.073 MTY, 0.083 MTY, and 0.1 MTY. It is observed that compared to low feedstock supply variability levels the unit cost of feedstock increases for high variability about 3.4%. This implies that the feedstock supply variability levels highly impact decision making in the feedstock supply chain network.

4.3.2. Impact of mean feedstock supply changes on system performance

The second set of experiments (shown in Fig. 11) show the impact of feedstock supply mean changes on feedstock supply chain network performance. There are a number of factors which impact the feedstock availability in a given region such as,

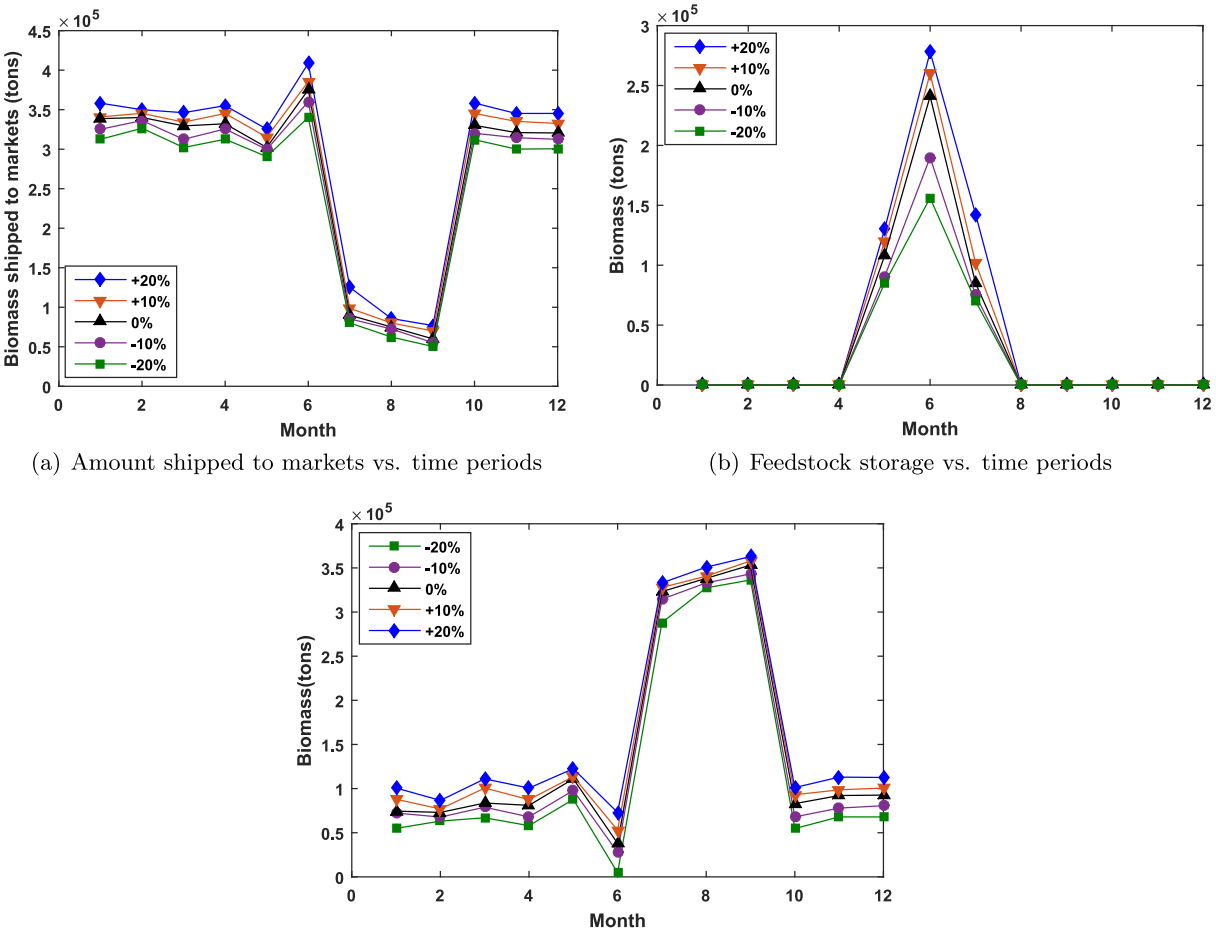

(a) Amount shipped to markets vs. time periods

(b) Feedstock storage vs. time periods

(c) Feedstock shortage vs. time periods

Fig. 11. Supply chain network decisions under different feedstock supply mean levels.

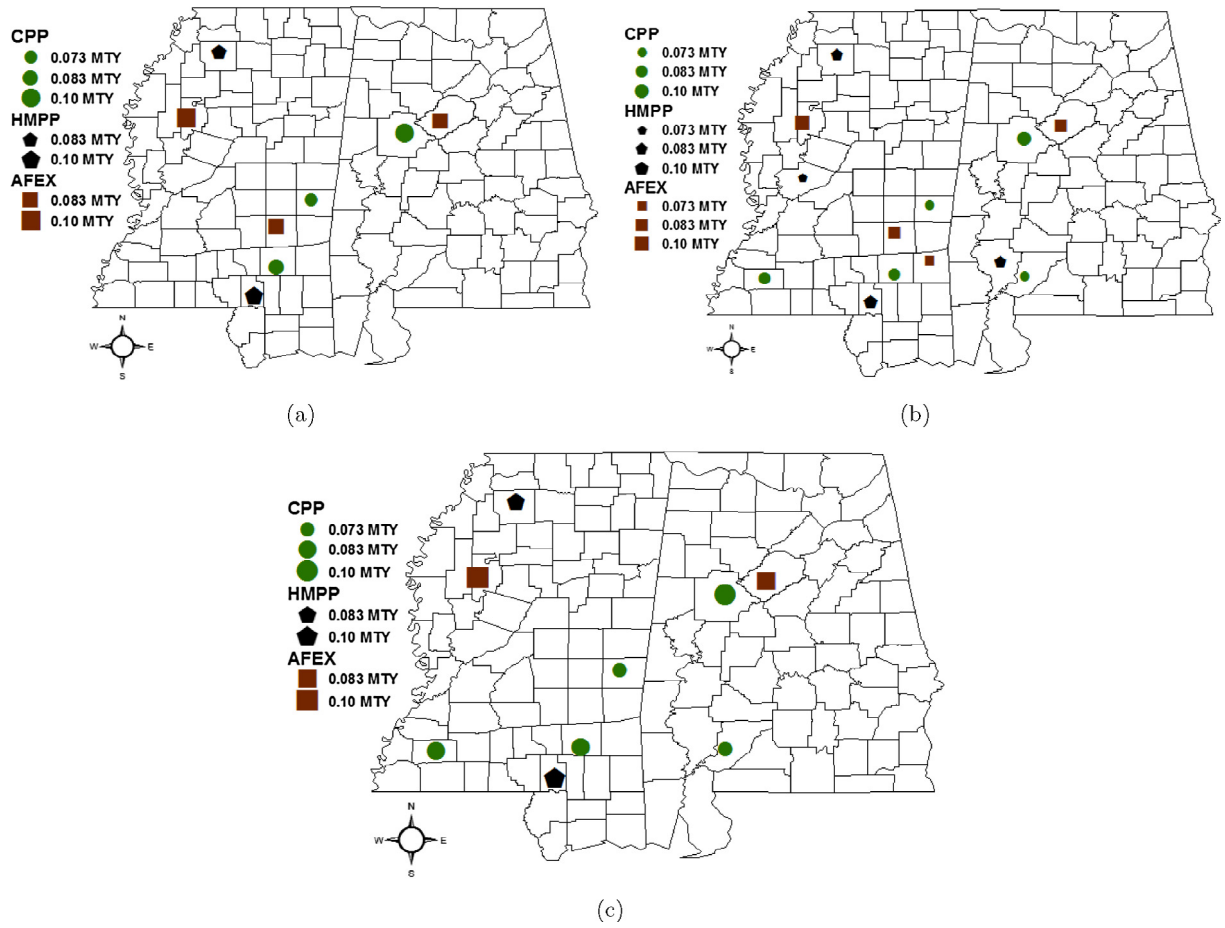

Fig. 12. Impact of mean feedstock supply changes on network configuration for (a) base case, (b) 20% increment of mean supply levels, and (c) 20% decrease of mean supply levels.

unexpected natural catastrophe, new initiatives from the government to promote cultivation of more feedstock or other related factors (Marufuzzaman et al., 2016). From Fig. 11, it is evident that if the supply mean is shifted positively (+20% or +10%) from the base case, then overall shipment from depot to market will also increase and vice versa. The same case is valid for feedstock storage over a time period. We notice that depots tend to store more feedstock during the off production period from December to February when none of the feedstock is available to maintain uniformly high feedstock supply variability levels through the whole year; this triggers a decrease in the overall shortage of feedstock supply in market $k \in \mathscr{K}$ at time period $t \in \mathscr{T}$.

Fig. 12 presents the number of CPP, HMPP and AFEX depots network configurations for the base case, 20% increment of feedstock supply levels, and 20% decrease of feedstock supply levels. It is observed from Fig. 12(a) that three CPP, two HMPP, and three AFEX depots have been selected for the base case. For a 20% increment of feedstock supply from the mean levels, the model selects two additional CPP depots, two HMPP depots, and one AFEX depot (Fig. 12 (b)), whereas for a 20% decrease of feedstock supply from mean levels, the model decides to close one AFEX depot which has been selected for the base case (Fig. 12(c)). It is further observed that the low mean feedstock supply scenario (e.g., −20% feedstock supply change) increases the unit delivery cost of feedstock by 6.42% from the base case and alternatively if there exists a high mean feedstock supply scenario (e.g., 20% feedstock supply change), the unit delivery cost could have dropped by 5.78% from the base case.

4.3.3. Performance evaluation of stochastic and deterministic solution

To justify the importance of using a stochastic programming approach over a deterministic approach, this study solves model [**DP**] using both approaches and compares their solutions. To get the deterministic solution, we use the average biomass supply $\bar{s}_{bit} = s^{\omega}_{bit}/|\Omega|$ where s^{ω}_{bit} is obtained from the different supply scenarios in the stochastic programming approach. Fig. 13 shows the comparison of major supply chain decisions with and without considering feedstock supply uncertainty. It is evident from the results that an additional 12.49% increase in biomass shipment is possible in markets to cope with feedstock supply seasonality and uncertainty. Moreover, the model decides to store 40.9% additional feedstock at depot facilities between the months of October ($t = 5$) to December ($t = 7$) to maintain a smooth feedstock supply during the off production seasons. This results in an overall 15.3% decrease in feedstock shortage quantity which eventually decreases the total system costs. On average, the unit delivery cost of feedstock transportation drops by 8.17% if both the feedstock seasonality and uncertainty are taken into consideration. Fig. 14 demonstrates the network configuration for the deterministic and stochastic approaches. It is interesting to note that the stochastic programming approach selects almost 33.33% more depot facilities $|\mathbf{Y}|$ over the deterministic counterpart. This supports the notion that feedstock supply uncertainty possess a high impact on feedstock supply chain network decisions and illustrates that the use of a stochastic solution is superior over a deterministic solution.

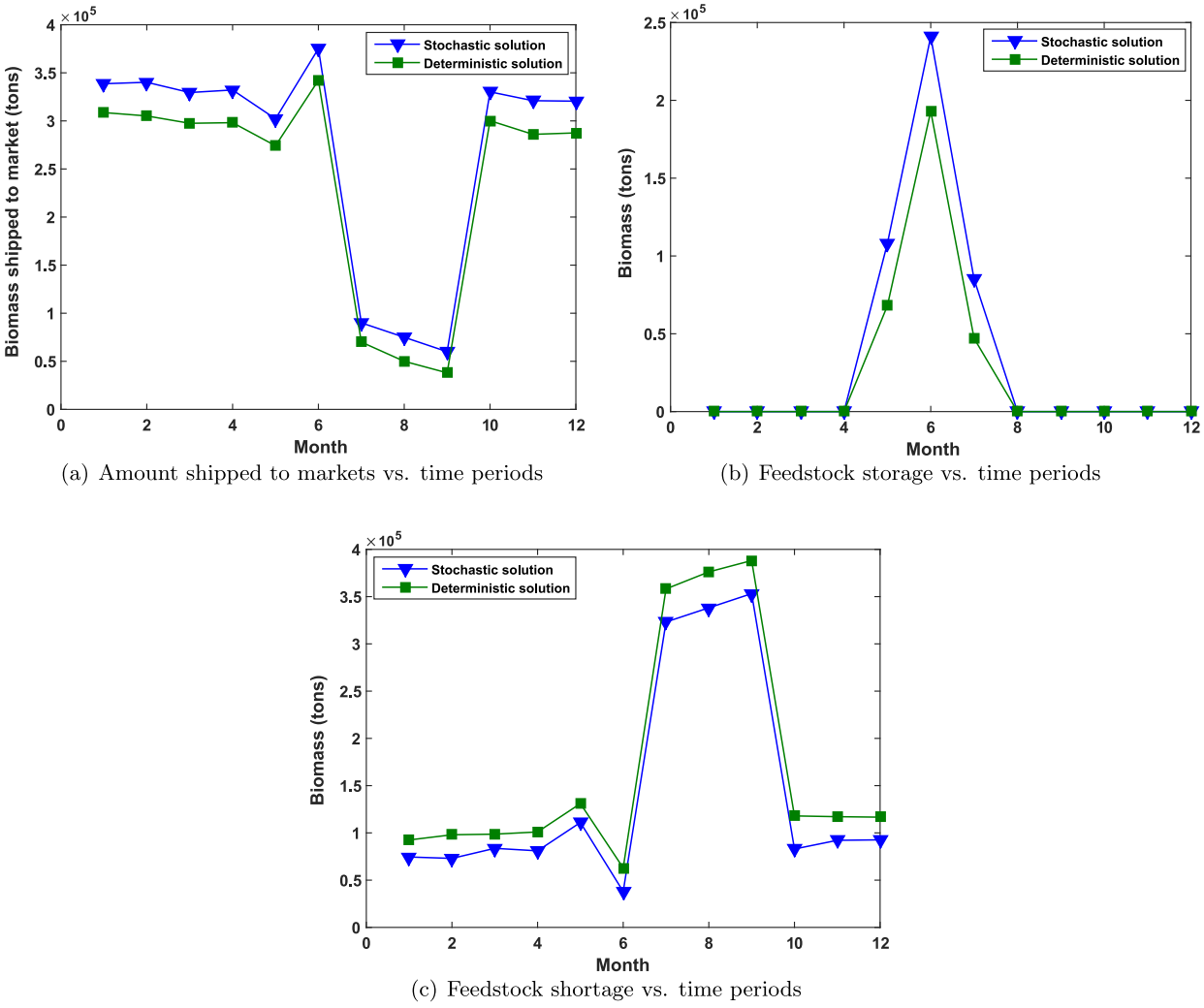

(a) Amount shipped to markets vs. time periods

(b) Feedstock storage vs. time periods

(c) Feedstock shortage vs. time periods

Fig. 13. Impact of stochastic vs. deterministic solution on system performance.

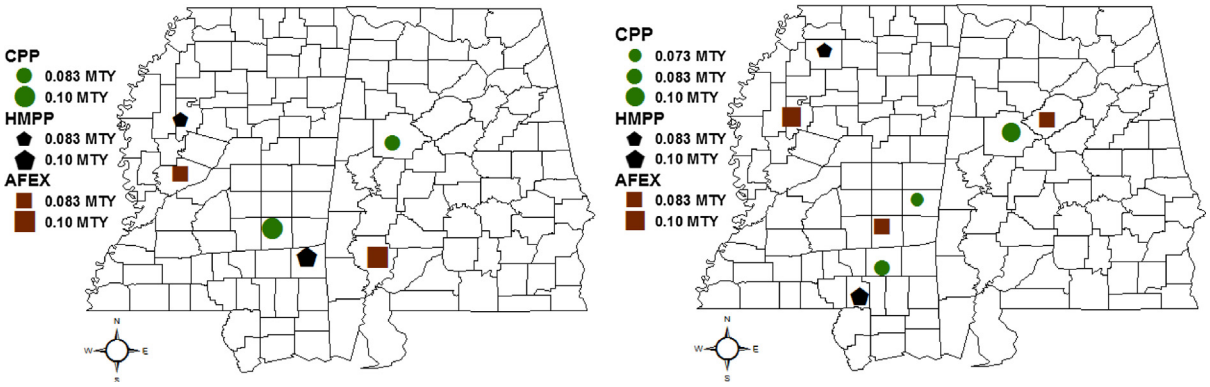

(a) Deterministic solution

(b) Stochastic solution

Fig. 14. Network representation with and without considering feedstock supply uncertainty.

4.3.4. Impact of feedstock supply variation levels with carbon emission on system performance

To see the impact of feedstock supply variation with carbon on a transportation network, we conducted a sensitivity analysis of the model **[EDP]**. Fig. 15 illustrates the distribution of depot facilities under low and high feedstock supply variability levels with carbon emission. It is observed from Fig. 15 that when the level of feedstock supply variation increases, the number of different types of depot facilities increases. More specifically, compared to low feedstock supply variability levels, an additional CPP depot of capacity 0.083 MTY, three additional HMPP depots of capacity 0.073 MTY, and two additional AFEX depots

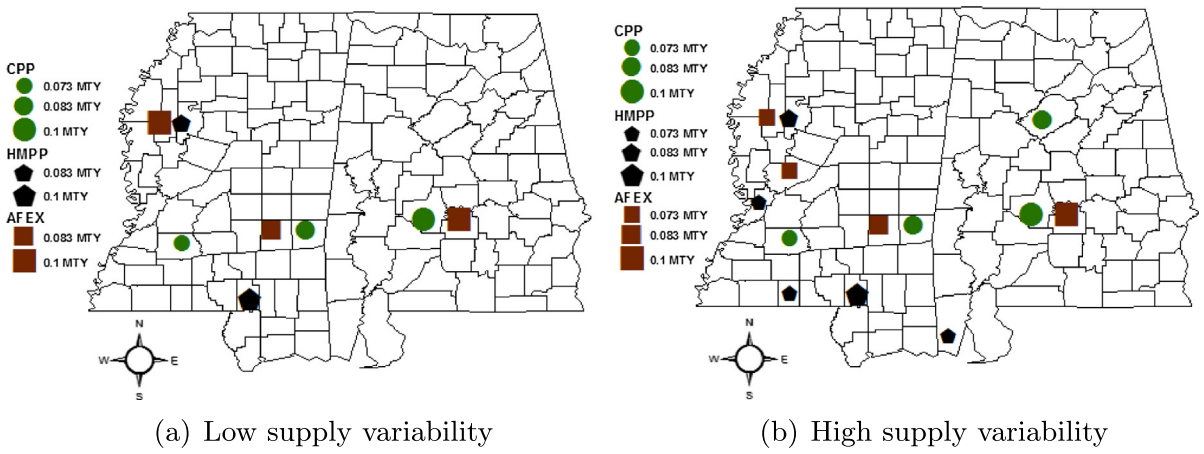

(a) Low supply variability (b) High supply variability

Fig. 15. Impact of feedstock supply variability with carbon emission on network configuration.

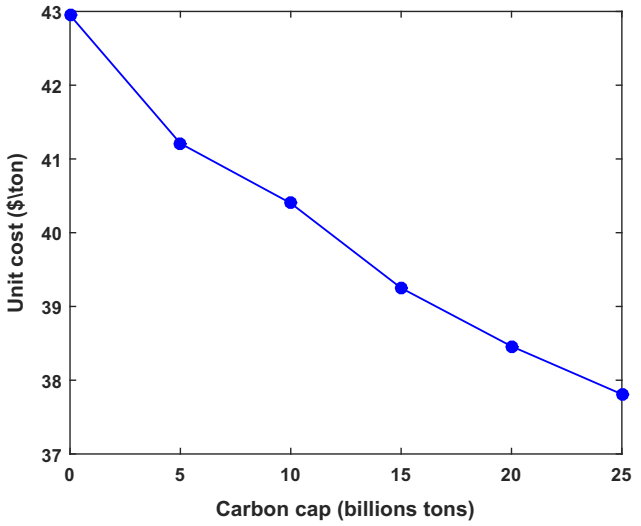

Fig. 16. Impact of carbon cap on feedstock unit price.

of capacities 0.073 MTY are selected to transport feedstock in markets in high feedstock supply variability levels. It is observed that high variation increases the unit cost of feedstock by 6.31% from the base case. We further notice that for both high and low variation of feedstock supply, the model decides to select the depot location near the supply and market location to reduce carbon emission.

4.3.5. Impact of carbon cap-and-trade mechanism on feedstock price

To recognize the impact of the carbon cap-and-trade mechanism on a feedstock supply chain network, we conducted a series of experiments changing the carbon cap. For our base, we have taken the carbon cap to be 10 billion tons per year. We have conducted 5 sets of experiments by setting the carbon cap at 5, 10, 15, 20, and 25 billion tons and keeping the same default setting for other parameters. Fig. 16 demonstrates that if the carbon credit is loose, the unit cost of the feedstock will be reduced. However, as the cap becomes tighter, the unit cost increases because at high carbon there is an incentive for the facilities to sell carbon credit to the market. When the carbon cap is loose, the feedstock supply chain networks can lower overall cost by selling the carbon credit to the market. On the other hand, as the carbon cap becomes tighter, the facilities are required to purchase additional carbon credit to maintain the supply chain activities resulting in higher supply chain costs. Results indicate that if the carbon cap is loosened from 10 billion tons per year to 25 billion tons per year, the unit feedstock cost will drop by 6.4%.

4.3.6. Sensitivity analysis of markets demand on system performance

We now present the impact of feedstock demand on the performance of the biomass supply chain network. Biomass is primarily used to fulfill the demands of bio-refineries and coal industries. However, we consider that processed feedstock (densified biomass) can also serve the demand of the pulp and paper and the animal feed markets. The results of the sensitivity analysis show that if the demand for feedstock of bio-refineries and coal industries decreases then the feedstock will be used by the pulp and paper industries and the animal feed markets. To perform the analysis, we conducted four different experiments: (a) 50% decreased demand of bio-refineries while keeping the demand fixed for the three other markets, (b) 50% decreased demand of coal industries while keeping the demand fixed for the three other markets, (c) 50% decreased demand of bio-refineries and coal industries while keeping the demand fixed for the three other markets, and (d) 50% decreased demand of bio-refineries and coal industries without the other two markets. Fig. 17 demonstrates the network representation under these four sets of experiment. It is obvious from the figure that the decrease in the demand from the bio-refineries and coal industries has a greater impact on making decisions related to open depots than the demand from the pulp and paper and animal feed markets. Specifically, for a 50% decrease in the bio-refineries demand, the model decides to open two CPP depots, two HMPP depots, and two AFEX depots (as shown in Fig. 17(a)) and for a 50% decrease in the coal industries demand, the model decides to open two CPP depots, two HMPP depots, and two AFEX depots (as shown in Fig. 17(b)). For a 50% decrease in the bio-refineries and coal industries demand, the model decides to open only two CPP depots, two HMPP depots, and one AFEX depot (as shown in Fig. 17(c)). We also observe that for a 50% decrease in the bio-refineries and coal industries demand and without considering pulp and paper and animal feed markets, the model decides to open only one CPP depot and two HMPP depots, while it has not decided to open any AFEX depots as shown in Fig. 17(d). In summary, we found that even though the demand of feedstock for bio-refineries and coal industries is decreased, the densified biomass can also be used to serve the pulp and paper and animal feed markets alternatively. These results indicate that development of multi-purpose pellet processing depots has a significant role in satisfying the multiple market demand for feedstock.

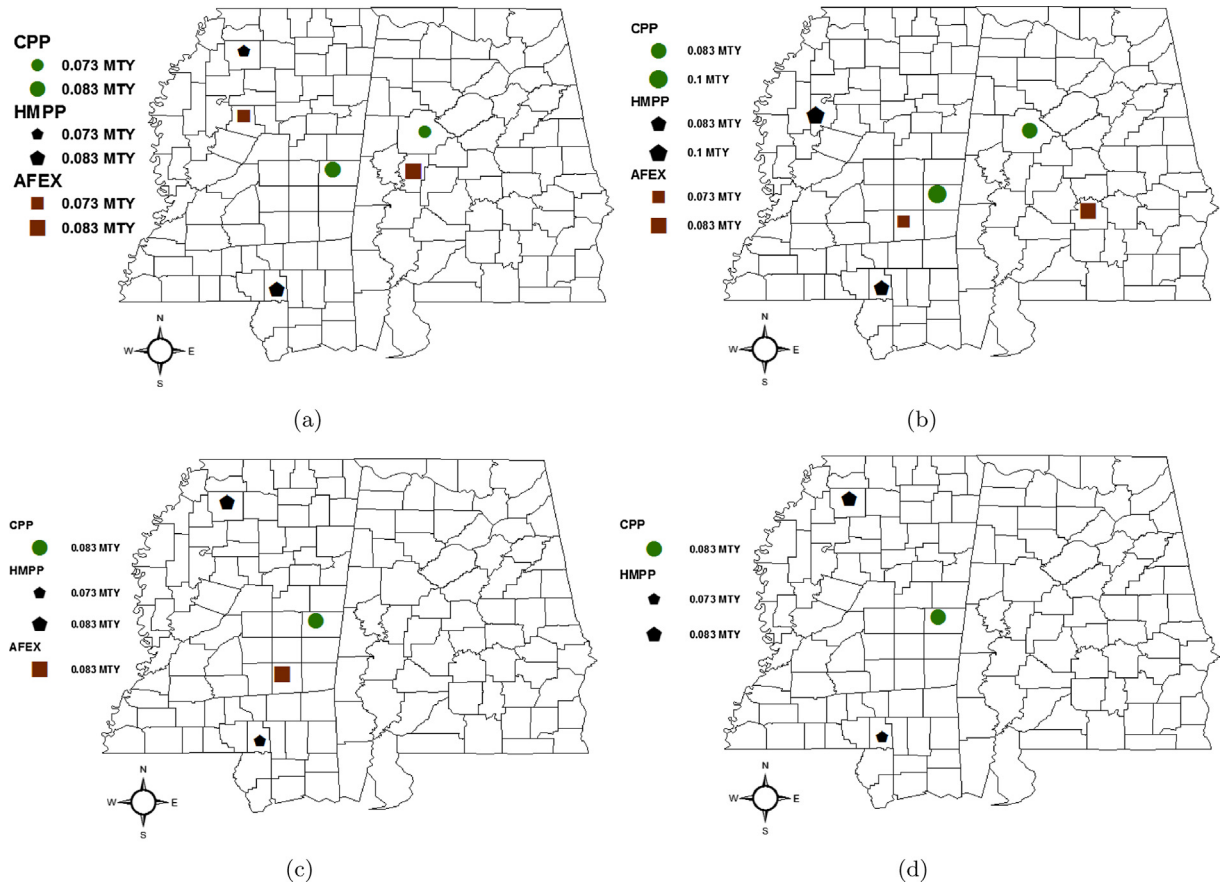

Fig. 17. Impact of demand decrease on network configuration by (a) 50% bio-refinery, (b) 50% coal industry, (c) 50% bio-refinery and coal industry, and (d) 50% bio-refinery and coal industry without the pulp and paper industry and animal feed market.

5. Conclusion

This paper studies the impact of feedstock supply uncertainty on the design and management of supply chain networks in multi-purpose pellet processing depots. This study is further extended to **[EDP]** by incorporating carbon emissions into consideration. A two-stage stochastic linear programming model not only determines the optimal size location and routing plan for multiple depot facilities for feedstock storage and processing plants, but also mitigates carbon emission from the supply chain network under feedstock supply uncertainty. We propose a hybrid algorithms that combine Sample Average Approximation algorithm with an enhanced Progressive Hedging algorithm to solve our proposed model. The enhanced Progressive Hedging algorithm combines several heuristics such as the dynamic penalty parameter updating technique, the local and global heuristic techniques, and the Rolling horizon algorithm. Computational results indicate that the hybrid decomposition algorithm (**SAA + PHA + HR + RH**) is capable of producing high quality feasible solution consistently in a reasonable amount of time to solve realistic large-size problem instances.

We use Mississippi and Alabama as a testing ground to evaluate the performance of the modeling results for our study. Our computational experiments reveal some insights into the impact of feedstock supply uncertainty on the design and management of supply chain networks in multi-purpose pellet processing depots. It is observed that depots can help to handle supply variation and that bio-refineries and coal industries will greatly benefit by the depots because when there is excess supply, the depots can sell excess feedstock to other markets. When there is a lesser supply, the depots can help to meet demand from their stored inventories. It is also observed that high supply variability increases the unit delivery cost of feedstock by 3.4% from the base case for model **[DP]** and by 6.31% for the model **[EDP]**. Furthermore, when the mean feedstock supply increases (e.g., 20%) it will drop the unit delivery cost of pelletized feedstock by 5.78% from the base case, and when the carbon credit is loose (25 billion tons), it will drop the unit delivery cost by 6.4% from the base case. The sensitivity analysis further reveals how feedstock demand on different markets affect the location and performance of the biomass supply chain network.

The contribution of this paper to the body of knowledge in supply chain can be summarized as follows:

- We propose a two-stage stochastic linear programming model for the design and management of supply chain networks in multi-purpose pellet processing depots.
- We develop a hybrid algorithm to solve the mathematical model. The proposed hybrid decomposition algorithm connects a Sample Average Approximation algorithm with an enhanced Progressive Hedging algorithm to make the model consistently solve faster and produce high quality solutions in a reasonable amount of time.
- A real-world case study of the model is presented to validate the effectiveness of the proposed hybrid algorithm. The findings from this study can be used by decision makers to design a robust logistics network for multi-purpose pellet processing depots.

This work can be extended in several directions. Since this study ignores the impact of congestion caused by feedstock seasonality

and uncertainty, future studies could address this issue. Furthermore, this work assumes that the feedstock supply chain network is robust and will never fail when in reality, the facilities can be disrupted due to natural (e.g., 2005 hurricane Katrina, 2008 China Haiti earthquake) or human-made disasters (e.g., 2010 gulf of Mexico oil spill). Future research factoring in the effect of natural or man-made disasters could add valuable information to the current work.

References

An, H., Wilhelm, W. E., & Searcy, S. W. (2011). A mathematical model to design a lignocellulosic biofuel supply chain system with a case study based on a region in Central Texas. *Bioresource Technology, 102*(17), 7860–7870.

Argo, A. M., Tan, E. C., Inman, D., Langholtz, M. H., Eaton, L. M., Jacobson, J. J., & Graham, R. L. (2013). Investigation of biochemical biorefinery sizing and environmental sustainability impacts for conventional bale system and advanced uniform biomass logistics designs. *Biofuels, Bioproducts and Biorefining, 7*(3), 282–302.

Atamturk, A., & Zhang, M. (2007). Two-stage robust network flow and design under demand uncertainty. *Operations Research, 55*(4), 662–673.

Awudu, I., & Zhang, J. (2012). Uncertainties and sustainability concepts in biofuel supply chain management: A review. *Renewable and Sustainable Energy Reviews, 16*(2), 1359–1368.

Awudu, I., & Zhang, J. (2013). Stochastic production planning for a biofuel supply chain under demand and price uncertainties. *Applied Energy, 103*, 189–196.

Balasubramanian, J., & Grossmann, I. (2004). Approximation to multistage stochastic optimization in multiperiod batch plant scheduling under demand uncertainty. *Industrial and Engineering Chemistry Research, 43*(14), 3695–3713.

Bals, B. D., & Dale, B. E. (2012). Developing a model for assessing biomass processing technologies within a local biomass processing depot. *Bioresource Technology, 106*, 161–169.

Barbarosoglu, G., & Arda, Y. (2004). A two-stage stochastic programming framework for transportation planning in disaster response. *Journal of the Operational Research Society, 55*(1), 43–53.

Bioenergy Knowledge Discovery Framework (KDF) (2016). Available from: <https://bioenergykdf.net/billionton2016/4/1/tableau>.

Bruglieri, M., & Liberti, L. (2008). Optimal running and planning of a biomass-based energy production process. *Energy Policy, 36*(7), 2430–2438.

Carolan, J. E., Joshi, S. V., & Dale, B. E. (2007). Technical and financial feasibility analysis of distributed bioprocessing using regional biomass pre-processing centers. *Journal of Agricultural & Food Industrial Organization, 5*(2), 10.

Chai, L., & Saffron, C. M. (2016). Comparing pelletization and torrefaction depots: Optimization of depot capacity and biomass moisture to determine the minimum production cost. *Applied Energy, 163*, 387–395.

Chen, C. W., & Fan, Y. (2012). Bioethanol supply chain system planning under supply and demand uncertainties. *Transportation Research Part E: Logistics and Transportation Review, 48*(1), 150–164.

Crainic, T. G., Fu, X., Gendreau, M., Rei, W., & Wallace, S. W. (2011). Progressive hedging-based metaheuristics for stochastic network design. *Networks, 58*, 114–124.

Dutta, A., Talmadge, M., Hensley, J., Worley, M., Dudgeon, D., Barton, D., ... Hess, J. (2011). *Process design and economics for conversion of lignocellulosic biomass to ethanol thermochemical pathway by indirect gasification and mixed alcohol synthesis*. National Renewable Energy Laboratory.

Eksioglu, S. D., Acharya, A., Leightley, L. E., & Arora, S. (2009). Analyzing the design and management of biomass-to-biorefinery supply chain. *Computers & Industrial Engineering, 57*, 1342–1352.

Eranki, P. L., & Dale, B. E. (2011). Comparative life cycle assessment of centralized and distributed biomass processing systems combined with mixed feedstock landscapes. *GCB Bioenergy, 3*(6), 427–438.

Eranki, P. L., Bals, B. D., & Dale, B. E. (2011). Advanced regional biomass processing depots: A key to the logistical challenges of the cellulosic biofuel industry. *Biofuels, Bioproducts and Biorefining, 5*(6), 621–630.

Gebreslassie, B. H., Yao, Y., & You, F. (2012). Design under uncertainty of hydrocarbon biorefinery supply chains: Multiobjective stochastic programming models, decomposition algorithm, and a comparison between CVaR and downside risk. *AIChE Journal, 58*(7), 2155–2189.

General Algebraic Modeling System (GAMS) (2013). Available from: <http://www.gams.com/>.

GHG Protocol (2015). Emission factors from cross-sector tools. <http://www.ghgprotocol.Org/calculation-tools/all-tools/>.

Gul, S., Denton, B. T., & Fowler, J. W. (2015). A progressive hedging approach for surgery planning under uncertainty. *INFORMS Journal on Computing, 27*(4), 755–772.

Hess, J. R., Wright, C. T., Kenney, K. L., & Searcy, E. M. (2009). *Uniform-format solid feedstock supply system: A commodity-scale design to produce an infrastructure-compatible bulk solid from lignocellulosic biomass – Executive summary*. Idaho National Laboratory.

Huang, Y., Chen, C. W., & Fan, Y. (2010). Multistage optimization of the supply chains of biofuels. *Transportation Research Part E, 46*(6), 820–830.

Huang, Y., Fan, Y., & Chen, C-W. (2014). An integrated biofuel supply chain to cope with feedstock seasonality and uncertainty. *Transportation Science, 48*(4), 540–554.

Hvattum, L. M., & Lokketangen, A. (2009). Using scenario trees and progressive hedging for stochastic inventory routing problems. *Journal of Heuristics, 15*, 527–557.

Kara, S. S., & Onut, S. (2010). A two-stage stochastic and robust programming approach to strategic planning of a reverse supply network: The case of paper recycling. *Expert Systems with Applications, 37*(9), 6129–6137.

Kim, J., Realff, M. J., & Lee, J. H. (2011). Optimal design and global sensitivity analysis of biomass supply chain networks for bio-fuels under uncertainty. *Computers & Chemical Engineering, 35*, 1738–1751.

Kim, J., Realff, M. J., Lee, J. H., Whittaker, C., & Furtner, L. (2011). Design of biomass processing network for biofuel production using an MILP model. *Biomass and Bioenergy, 35*(2), 853–871.

Kleywegt, A. J., Shapiro, A., & Homem-De-Mello, T. (2001). The sample average approximation method for stochastic discrete optimization. *SIAM Journal of Optimization, 12*, 479–502.

Kostina, A. M., Guillen-Gosalbeza, G., Meleb, F. D., Bagajewiczc, M. J., & Jimeneza, L. (2011). A novel rolling horizon strategy for the strategic planning of supply chains. Application to the sugar cane industry of Argentina. *Computers & Chemical Engineering, 35*, 2540–2563.

Lamers, P., Roni, M. S., Tumuluru, J. S., Jacobson, J. J., Cafferty, K. G., Hansen, J. K., ... Bals, B. (2015). Techno-economic analysis of decentralized biomass processing depots. *Bioresource Technology, 194*, 205–213.

Li, J. M., Li, A. H., Varbanov, P. S., & Liu, Z. Y. (2017). Distance potential concept and its applications to the design of regional biomass supply chains and solving vehicle routing problems. *Journal of Cleaner Production*.

Li, X., Peng, F., Bai, Y., & Ouyang, Y. (2015). Effects of disruption risks on biorefinery location design: Discrete and continuous models. In *Proceeding of the 90th TRB annual meeting, Washington D.C.*. .

Magnanti, T. L., & Wong, R. T. (1981). Accelerating Benders Decomposition: Algorithmic enhancement and model selection criteria. *Operations Research, 29*, 464–484.

Maheshwari, P., Singla, S., & Shastri, Y. (2017). Resiliency optimization of biomass to biofuel supply chain incorporating regional biomass pre-processing depots. *Biomass and Bioenergy, 97*, 116–131.

Mak, W. K., Morton, D. P., & Wood, R. K. (1999). Monte Carlo bounding techniques for determining solution quality in stochastic programs. *Operations Research Letters, 24*, 47–56.

Marufuzzaman, M., & Eksioglu, S. D. (2016). Designing a reliable and dynamic multi-modal transportation network for biofuel supply chain. *Transportation Science*. http://dx.doi.org/10.1287/trsc.2015.0632 (in press).

Marufuzzaman, M., Eksioglu, S. D., & Huang, Y. (2014). Two-stage stochastic programming supply chain model for biodiesel production via wastewater treatment. *Computers and Operations Research, 49*, 1–17.

Marufuzzaman, M., Li, X., Yu, F., & Zhou, F. (2016). Supply chain design and management for syngas production. *ACS Sustainable Chemistry & Engineering, 4*(3), 890–900.

Memisoglu, G., & Uster, H. (2015). Integrated bio-energy supply chain network planning problem. *Transportation Science* (in press).

Vogel, K., Schmer, M., & Mitchell, R. (2010). Switchgrass (panicum virgatum) for biofuel production. Available from: <http://extension.org/pages/Switchgrass_for_Biofuel_Production>.

Mulvey, J. M., & Vladimirou, H. (1991). Applying the progressive hedging algorithm to stochastic generalized networks. *Annals of Operations Research, 31*, 399–424.

Ng, R. T., & Maravelias, C. T. (2015). Design of cellulosic ethanol supply chains with regional depots. *Industrial & Engineering Chemistry Research, 55*(12), 3420–3432.

Ng, R. T., & Maravelias, C. T. (2017). Design of biofuel supply chains with variable regional depot and biorefinery locations. *Renewable Energy, 100*, 90–102.

Norkin, V. I., Ermoliev, Y. M., & Ruszczynski, A. (1998). On optimal allocation of indivisibles under uncertainty. *Operations Research, 46*, 381–395.

Norkin, V. I., Pflug, G. C., & Ruszczynski, A. (1998). A branch and bound method for stochastic global optimization. *Mathematical Programming, 83*(3), 425–450.

Parker, N., Tittmann, P., Hart, Q., Lay, M., Cunningham, J., Jenkins, B., & Schmidt, A. (2008). *Strategic assessment of bioenergy development in the west: Spatial analysis and supply curve development*. Western Governors Association.

Parkhurst, K. M., Saffron, C. M., & Miller, R. O. (2016). An energy analysis comparing biomass torrefaction in depots to wind with natural gas combustion for electricity generation. *Applied Energy, 179*, 171–181.

Poudel, S., Marufuzzaman, M., & Bian, L. (2016a). A hybrid decomposition algorithm for designing a multi-modal transportation network under biomass supply uncertainty. *Transportation Research Part E, 94*, 1–25.

Poudel, S., Marufuzzaman, M., & Bian, L. (2016b). Designing a reliable biofuel supply chain network considering link failure probabilities. *Computers and Industrial Engineering, 91*, 85–99.

Qi, Y., & Sen, S. (2017). The Ancestral Benders cutting plane algorithm with multi-term disjunctions for mixed-integer recourse decisions in stochastic programming. *Mathematical Programming, 161*(1-2), 193–235.

Rajgopal, J., Wang, Z., Schaefer, A. J., & Prokopyev, O. A. (2011). Integrated design and operation of remnant inventory supply chains under uncertainty. *European Journal of Operational Research, 214*(2), 358–364.

Rockafellar, R. T., & Wets, R. J.-B. (1991). Scenarios and policy aggregation in optimization under uncertainty. *Mathematics of Operations Research, 16*, 119–147.

Roni, M. S., Eksioglu, S. D., Searcy, E., & Jha, K. (2014). A supply chain network design model for biomass co-firing in coal-fired power plants. *Transportation Research Part E, 61*, 115–134.

Rudolfsson, M., Stelte, W., & Lestander, T. A. (2015). Process optimization of combined biomass torrefaction and pelletization for fuel pellet production. A parametric study. *Applied Energy, 140*, 378–384.

Santoso, T., Ahmed, S., Goetschalckx, M., & Shapiro, A. (2005). A stochastic programming approach for supply chain network design under uncertainty. *European Journal of Operational Research, 167*, 96–115.

Schutz, P., Tomasgard, A., & Ahmed, S. (2009). Supply chain design under uncertainty using sample average approximation and dual decomposition. *European Journal of Operational Research, 199*, 409–419.

Shapiro, A. (2005). Complexity of two and multi-stage stochastic programming problems. *Tutorial Notes for School of Industrial and Systems Engineering*, 1–27.

Simic, V. (2016). End-of-life vehicles allocation management under multiple uncertainties: An interval-parameter two-stage stochastic full-infinite programming approach. *Resources, Conservation and Recycling, 114*, 1–17.

Teymouri, F., Laureano-Perez, L., Alizadeh, H., & Dale, B. E. (2005). Optimization of the ammonia fiber explosion (AFEX) treatment parameters for enzymatic hydrolysis of corn stover. *Biosource Technology, 96*(18), 2014–2018.

United States Energy Information Administration (2015). State energy data system (seds): 2012 (updates). <http://www.eia.gov/state/seds/seds-data-fuel.cfm?sid=US>.

US Environmental Protection Agency (2015). <http://www.epa.gov/cleanenergy/energy-resources/refs.html>.

Verweij, B., Ahmed, S., Kleywegt, A. J., Nemhauser, G., & Shapiro, A. (2003). The sample average approximation method applied to stochastic routing problems: A computational study. *Computational Optimization and Applications, 24*, 289–333.

Wallace, S. W., & Helgason, T. (1991). Structural properties of the progressive hedging algorithm. *Annals of Operations Research, 31*, 445–456.

Xie, W., & Ouyang, Y. (2013). Dynamic planning of facility locations with benefits from multi type facility colocation. *Computer-Aided Civil & Infrastructure Engineering, 28*(9), 666–678.

Zhang, F., Johnson, D. M., & Wang, J. (2016). Integrating multimodal transport into forest-delivered biofuel supply chain design. *Renewable Energy, 93*, 58–67.